

1 Hunga Tonga-Hunga Ha'apai Volcano Impact Model

2 Observation Comparison (HTHH-MOC) Project:

3 Experiment Protocol and Model Descriptions

4
5 Yunqian Zhu^{1,2}, Hideharu Akiyoshi³, Valentina Aquila⁴, Elisabeth Asher^{1,5}, Ewa M. Bednarz^{1,2},
6 Slimane Bekki⁶, Christoph Brühl⁷, Amy H. Butler², Parker Case⁸, Simon Chabrillat⁹, Gabriel
7 Chiodo¹⁰, Margot Clyne^{11,12}, Peter R. Colarco^{8,37}, Sandip Dhomse¹⁸, Lola Falletti⁶, Eric
8 Fleming^{8,13}, Ben Johnson³⁸, Andrin Jörmann^{10,36}, Mahesh Kovilakam¹⁵, Gerbrand Koren¹⁶, Ales
9 Kuchar¹⁷, Nicolas Lebas¹⁴, Qing Liang⁸, Cheng-Cheng Liu¹², Graham Mann¹⁸, Michael
10 Manyin^{8,13}, Marion Marchand⁶, Olaf Morgenstern^{19,20*}, Paul Newman⁸, Luke D. Oman⁸, Freja F.
11 Østerstrøm^{21,22}, Yifeng Peng²³, David Plummer²⁴, Iaria Quaglia²⁵, William Randel²⁵, Samuel
12 Rémy²⁶, Takashi Sekiya²⁷, Stephen Steenrod^{8,28}, Timofei Sukhodolov³⁶, Simone Tilmes²⁵, Kostas
13 Tsigaridis^{29,30}, Rei Ueyama³¹, Daniele Visioni³², Xinyue Wang¹¹, Shingo Watanabe²⁷, Yousuke
14 Yamashita³, Pengfei Yu³³, Wandu Yu³⁴, Jun Zhang²⁵, Zhihong Zhuo³⁵

- 15
- 16 1. Cooperative Institute for Research in Environmental Sciences (CIRES), University of
- 17 Colorado Boulder, USA
- 18 2. NOAA Chemical Sciences Laboratory, Boulder, USA
- 19 3. National Institute for Environmental Studies, Tsukuba, Japan
- 20 4. American University, Department of Environmental Science, Washington, DC, USA
- 21 5. NOAA Global Monitoring Laboratory, Boulder, USA
- 22 6. LATMOS, UVSQ, CNRS, INU, Sorbonne Université, Paris, France
- 23 7. Max Planck Institute for Chemistry, Mainz, Germany
- 24 8. NASA Goddard Space Flight Center, Maryland, USA
- 25 9. Royal Belgian Institute for Space Aeronomy (BIRA-IASB), Brussels, Belgium
- 26 10. Institute for Atmospheric and Climate Science, ETH Zurich, Zurich, Switzerland; Instituto de
- 27 Geociencias, Spanish National Research Council (IGEO-CSIC-UCM), Madrid
- 28 11. Department of Atmospheric and Oceanic Sciences, University of Colorado Boulder, Boulder,
- 29 USA
- 30 12. LASP, University of Colorado Boulder, Boulder, USA
- 31 13. Science Systems and Applications, Inc., Lanham, MD, USA
- 32 14. LOCEAN/IPSL, Sorbonne Université, CNRS, IRD, MNHN, Paris, France
- 33 15. NASA Langley Research Center, VA, USA
- 34 16. Copernicus Institute of Sustainable Development, Utrecht University, Utrecht, Netherlands
- 35 17. BOKU University, Vienna, Austria
- 36 18. School of Earth and Environment, University of Leeds; UK National Centre for Atmospheric
- 37 Science, University of Leeds, Leeds, UK
- 38 19. National Institute of Water and Atmospheric Research (NIWA), Wellington, New Zealand
- 39 20. School of Physical and Chemical Sciences, University of Canterbury, Christchurch, New
- 40 Zealand
- 41 21. School of Engineering and Applied Sciences, Harvard University, Cambridge, MA, USA
- 42 22. Department of Chemistry, University of Copenhagen, Copenhagen, Denmark
- 43 23. Lanzhou University, Lanzhou, China
- 44 24. Climate Research Division, Environment and Climate Change Canada, Montréal, Canada

- 45 25. NCAR ACOM, Boulder, USA
46 26. HYGEOS, Lille, France
47 27. Japan Agency for Marine-Earth Science and Technology (JAMSTEC), Yokohama, Japan
48 28. University of Maryland-Baltimore County, Baltimore, MD, USA
49 29. Center for Climate Systems Research, Columbia University, New York, NY, USA.
50 30. NASA Goddard Institute for Space Studies, New York, NY, USA.
51 31. NASA Ames Research Center, Moffett Field, CA
52 32. Department of Earth and Atmospheric Sciences, Cornell University, Ithaca, NY
53 33. Jinan University, Guangzhou, China
54 34. Lawrence Livermore National Laboratory, USA
55 35. Department of Earth and Atmospheric Sciences, University of Quebec in Montreal, Montreal
56 (Quebec), Canada
57 36. Physikalisch-Meteorologisches Observatorium Davos and World Radiation Center, Davos,
58 Switzerland
59 37. Earth System Science Interdisciplinary Center, University of Maryland, College Park, MD
60 USA
61 38. Met Office Hadley Centre, Exeter, UK

62
63

64 * now at: German Meteorological Service (DWD), Offenbach, Germany

65
66

67 Correspondence to: Yunqian Zhu yunqian.zhu@colorado.edu

68

69 **Abstract:**

70

71 The 2022 Hunga volcanic eruption injected a significant amount of water vapor and a moderate
72 amount of sulfur dioxide into the stratosphere causing observable responses in the climate
73 system. We have developed a model-observation comparison project to investigate the evolution
74 of volcanic water and aerosols, and their impacts on atmospheric dynamics, chemistry, and
75 climate, using several state-of-the-art chemistry climate models. The project goals are: 1.

76 Evaluate the current chemistry-climate models to quantify their performance in comparison to
77 observations; and 2. Understand atmospheric responses in the Earth system after this exceptional
78 event and investigate the potential impacts in the projected future. To achieve these goals, we
79 designed specific experiments for direct comparisons to observations, for example from balloons
80 and the Microwave Limb Sounder satellite instrument. Experiment 1 consists of two sets of free-
81 running ensemble experiments from 2022 to 2031: one with fixed sea-surface temperatures and
82 sea-ice, and one with coupled ocean. These experiments will help to: understand the long-term
83 evolution of water vapor and aerosols; quantify HTHH effects on stratospheric and mesospheric
84 temperatures, dynamics, and transport; understand the impact of dynamic changes on ozone
85 chemistry; quantify the net radiative forcings; and evaluate any surface climate impact.

86 Experiment 2 is a nudged-run experiment from 2022 to 2023 using observed meteorology. To
87 allow participation of more climate models with varying complexities of aerosol simulation, we
88 include two sets of simulations in Experiment 2: Experiment 2a is designed for models with
89 internally-generated aerosol while Experiment 2b is designed for models using prescribed
90 aerosol surface area density. This experiment will help to: analyze H₂O & aerosol evolution;

91 quantify the net radiative forcings; understand the impacts on mid-latitude and polar O₃
92 chemistry as well as allow close comparisons with observations.

93

94 **1. Introduction and motivations of this project**

95

96 The Hunga Tonga-Hunga Ha'apai (HTHH) Impacts activity was established in the World
97 Climate Research Programme (WCRP) Atmosphere Processes And their Role in Climate
98 (APARC) as a limited-term focused cross-activity with a duration of three years. It aims to assess
99 the impacts of the 15 January 2022 Hunga volcanic eruption and produce an assessment to
100 document the Hunga impact on the climate system. The Hunga eruption injected an
101 unprecedented amount of water (H₂O) and moderate sulfur dioxide (SO₂) into the stratosphere
102 (Millan et al., 2022), presenting a unique opportunity to understand the impacts on the
103 stratosphere of a large-magnitude explosive phreatomagmatic eruption. The wide range of
104 satellite observations of the stratospheric water and sulfate plumes, global transport and
105 dispersion of volcanic materials, and unusual chemical and temperature signals are helpful in
106 assessing model representations of stratospheric chemistry, aerosol, and dynamics. For example,
107 the Aura Microwave Limb Sounder (MLS) observed ~150 Tg of water injected by the Hunga
108 eruption (Millan et al., 2022), which slowly decayed due to the polar stratospheric cloud (PSC)
109 dehydration process and stratosphere-troposphere exchange (Fleming et al., 2024; Zhou et al.,
110 2024). Large aerosol optical depth is observed by Ozone Mapping and Profiler Suite (OMPS)
111 (Taha et al., 2022), due to fast formation of sulfate (Zhu et al., 2022) and the high optical
112 efficiency of Hunga aerosol particles (Li et al., 2024). Unlike the stratospheric warming patterns
113 observed from previous large volcanic eruptions (El Chichón in 1982 and Pinatubo in 1991),
114 global stratospheric temperatures decreased by 0.5 to 1.0 K in the first two years following the
115 Hunga eruption, largely due to radiative cooling from injected water vapor (Randel et al., 2024).
116 Satellite observations in June, July, August 2022 reveal reduced lower stratospheric ozone (O₃)
117 over the SH midlatitudes and subtropics, with high levels near the equator, exceeding previous
118 variability. These ozone anomalies coincide with a weakening of the Brewer-Dobson circulation
119 during this period (Wang et al., 2023). Changes in stratospheric winds also influence the
120 mesosphere, leading to a stronger mesospheric circulation and corresponding temperature
121 changes (Yu et al., 2023). These observed phenomena provide a unique opportunity to test the
122 ability of chemistry-climate models to simulate the evolution of volcanic aerosols combined with
123 such a large amount of water vapor, as well as understand how volcanic water vapor and aerosols
124 modify radiative balances and stratospheric ozone.

125 The APARC HTHH Impacts activity aims to provide a benchmark analysis of the
126 eruption impacts so far, and projections of eruption climate impacts over the next few years. Two
127 multi-model evaluation projects are designed to facilitate the success of this activity: Tonga
128 Model Intercomparison Project (Tonga-MIP) (Clyne et al. 2024) and the Hunga Tonga-Hunga
129 Ha'apai Volcano Impact Model Observation Comparison (HTHH-MOC) Project (this paper).
130 The HTHH-MOC provides a foundation for a coordinated multi-model evaluation of global
131 chemistry-climate models' performance in response to the Hunga volcanic eruption. It defines a
132 set of perturbation experiments, where volcanic forcings—injecting water vapor and aerosol
133 concentrations—are consistently applied across participating model members. HTHH-MOC
134 aims to assess how reliably global chemistry-climate models simulate the climate responses to
135 this unprecedented volcanic forcing. This project enhances our confidence in attributing and
136 interpreting observations following the Hunga eruption. The scientific questions related to the

137 HTHH-MOC are: How does the Hunga volcanic plumes' transport relate to or impact
138 stratospheric dynamics (such as Brewer-Dobson circulation, polar vortex and the Quasi-Biennial
139 Oscillation) and upper atmosphere? What are the chemical impacts of the Hunga eruption in the
140 stratosphere and mesosphere? What and how long is the radiative effect of the Hunga eruption?
141 Does Hunga impact the tropospheric/surface climate?

142 Therefore, the HTHH-MOC project is focused on evaluating global chemistry-climate
143 models regarding the following three science themes: (1) plume evolution, dispersion, and large-
144 scale transport; (2) impacts on stratospheric chemistry and the ozone layer; and (3) radiative
145 effect from the eruption and surface climate impacts. Besides the HTHH-MOC project, the
146 assessment also includes analysis of observations and models that are not global climate models.
147 In the following paragraph, we describe the HTHH-MOC experiment design and participating
148 models.

149

150 2. Experiment Design

151 There are two experiments (**Exp1** and **Exp2** detailed below) designed to fulfill the
152 scientific goals. Each experiment includes a set of simulations with different volcanic injections
153 (i.e. with and without water and/or SO₂ injections), to explore the separate impacts of volcanic
154 water and aerosols during the post-eruption period: a) Control case (no eruption); b) H₂O (~150
155 Tg) & SO₂ (0.5 Tg); c) Only H₂O (~150 Tg). d) Only SO₂ (0.5 Tg). Simulations with the
156 injection of SO₂ only (d) are optional and designed for aerosol-focused models. The SO₂ and
157 water injections are prescribed based on Millan et al. (2022) and Carn et al. (2023). Note that
158 ~150 Tg of water is not the injection amount but the amount retained after the first couple of
159 days. This is because some models form ice particles that fall out of the stratosphere due to large
160 H₂O supersaturation during the initial injection (Zhu et al., 2022); these models will have to
161 inject more H₂O to counterbalance the ice formation (see **Table 6**). The only requirement is that
162 the model should have reasonable comparison to the MLS observations for water vapor as shown
163 in **Figure 1**. Aside from retaining ~150 Tg of water, the water vapor enhancement should be near
164 10 hPa to 50 hPa, and most of the water vapor should be located between 10°N and 30°S by
165 March 2022.

166 The first experiment (**Exp1**) is a free-running ensemble simulation covering the period
167 from 2022 to 2031. The experiment has been designed to answer questions on: 1. Understanding
168 the long-term evolution of Hunga water vapor and aerosols in free-running models; 2.
169 Quantifying Hunga effects on stratospheric temperatures, dynamics, and transport; 3.
170 Understanding the impact of dynamic changes on ozone chemistry; 4. Quantifying the net
171 radiative effects; 5. Estimating surface impacts (e.g., temperature, El Niño-Southern Oscillation,
172 monsoon precipitation, etc.). Simulations with free-running meteorology are required to properly
173 understand the impacts of the eruption on atmospheric dynamics and transport processes, and the
174 resulting impacts of those on chemical species (e.g., ozone) and surface climate. Since coupling
175 of the atmosphere with ocean and land processes is required to fully simulate many aspects of the
176 surface impacts, the use of coupled atmosphere, ocean, and land models is recommended.
177 However, since such a fully interactive set up imposes additional computing requirements, an
178 alternative model set up with fixed sea-surface temperatures (SSTs) and sea-ice is also allowed.
179 In that case, the prescribed climatological SSTs and sea-ice data are obtained by averaging SST
180 during the past decade (2012-2021), with the same data imposed in both the H₂O+SO₂ (b) and
181 control (a) simulations. It is important to note that both initial and boundary conditions in a
182 model come with uncertainties, and model processes are simplified. Therefore, model

183 simulations are influenced by the characteristics of the model itself and the background state of
184 the atmospheric system (Jones et al., 2016; Brodowsky et al., 2021). To address some of the
185 inherent uncertainties and reduce contribution of interannual variability to the forced response,
186 we use a large ensemble of simulations with slightly varied initial conditions. Note that in the
187 projection of stratospheric volcanic forcing, we only considered the Hunga eruption since 2022,
188 and no future explosive eruptions are included. For example, the 2024 Mt. Ruang eruption
189 contributed to elevated stratospheric aerosol optical depth, but it is not included.

190 Particularly, the first 5 years of qualified models output of **Exp1** are used to understand
191 climate impacts on the mesosphere and ionosphere from 2022-2027, such as gravity wave drag,
192 temperature changes, polar mesospheric clouds (PMCs), and atmospheric circulation. The
193 qualified models need to resolve the upper atmosphere with vertical resolutions higher or equal
194 to what we request in **Section 3**.

195 Since some aspects of the response, e.g., impacts on the radiative effect, may be too noisy
196 from free-running model simulations even with large ensembles, we have also designed the
197 second experiment which uses nudged temperature and meteorology to ensure that the
198 meteorology will be as close as possible to the one observed and thus isolate chemical changes
199 and their radiative effect. Experiment 2 (**Exp2**) is a two-year simulation that runs from 2022 to
200 2023 with nudged winds and/or temperature to answer questions on H₂O and aerosol evolution;
201 quantification of the net radiative effects; and impacts on mid-latitude and polar ozone
202 chemistry. **Exp2** has two distinct realizations: Experiment 2a (**Exp2a**) and Experiment 2b
203 (**Exp2b**). The models participating in **Exp2a** all have a prognostic aerosol module, but vary in
204 the complexity of their representation of aerosol microphysics (i.e., bulk, modal, or sectional).
205 Models participating in **Exp2b** use prescribed aerosol surface area density (SAD) and radiative
206 properties as input to the models (Jörmann, 2024). The prescribed aerosol properties are
207 calculated using Global Space-based Stratospheric Aerosol Climatology (GloSSAC; Thomason
208 et al., 2018; Kovilakam et al., 2020, 2023) version 2.22 aerosol data from 1979-2023. Note that
209 for the period after the Hunga eruption, GloSSAC uses the Stratospheric Aerosol and Gas
210 Experiment (SAGEIII/ISS) version 5.3 interpolated along the time axis and the Optical
211 Spectrograph and InfraRed Imager System (OSIRIS) version 7.3 to fill in any missing data
212 poleward of 60° N/S due to the unavailability of the Cloud-Aerosol Lidar and Infrared Pathfinder
213 Satellite Observations (CALIPSO) data since January 2022. Therefore, when conducting
214 analyses north/south of 60°N/S it should be noted that the aerosols may be underestimated due to
215 the OSIRIS instrument retrieval biases. We ask for the models to check their initial chemical
216 fields against MLS to see if the models are qualified to evaluate their ozone chemistry. The
217 nudged runs of **Exp2** enable isolation of the chemical impact of the Hunga eruption from the
218 volcanically induced changes in dynamics by comparing the runs with and without H₂O+SO₂
219 injection. The net radiative effect anomaly due to water and sulfate aerosol can also be calculated
220 by comparing the control run (a) with the H₂O+SO₂ injection run (b).

221 **Table 1** shows the forcings and emissions data used for the HTHH-MOC experiments.
222 **Table 2** shows the settings specific to each experiment. For volcanic injection for **Exp1** and **2**,
223 we recommend the injections of H₂O and SO₂ at 4 UTC on Jan 15, 2022. All the models are
224 required to retain a similar amount of water as observed by MLS (~ 150 Tg). The models are
225 recommended to compare with the MLS evolution for validation (**Figure 1**). The goal is to retain
226 the same amount of water and similar altitude to start with, so we can analyze the water's impact
227 on the stratosphere and climate. If injecting 25-30 km cannot retain 150 Tg, models can inject

228 higher than 30 km. The SO₂ injection is required to be 0.5 Tg for all models. The injection
 229 locations are not required to be co-injected with H₂O.

230 The data analysis of this project is designed to do inter-model comparisons, as well as
 231 inter-experiment comparisons. For example, the comparisons between **Exp2a** and **Exp2b** can
 232 help to understand how well we simulate the sulfate SAD and the importance of SAD variation
 233 for stratospheric ozone chemistry. Comparing **Exp1** and **Exp2** for the same period can help
 234 understand instantaneous and adjusted radiative effects. In addition, large (10-20) member
 235 ensembles are requested for free-running simulations to better quantify the role of internal
 236 variability in the climate response.

237

238 **Table 1. Summary of forcings and emissions data used in HTHH-MOC experiments.**

Spin-up*	5 years nudged runs
Degassing** and eruptive volcano source	Need both degassing and eruptive volcanic input for 5-year spin-up. Degassing continues during the experiment runs (e.g. 10 years for Exp1 , 2 years for Exp2). recommended references: Volcanic degassing Carn et al. (2017); Eruptive volcanoes (Neely III, & Schmidt (2016) https://archive.researchdata.leeds.ac.uk/96/ or Carn et al. (2017); Assume no more explosive volcanoes after Hunga.
Surface emission	Coupled Model Intercomparison Project phase 6 (CMIP6) emissions follow SSP2-4.5 (Gidden et al., 2019), which adopts an intermediate greenhouse gas (GHG) emission: CO ₂ emissions around current levels before beginning to decline by 2050.
Chemical initialization	Stratospheric chemistry fields (such as O ₃ , H ₂ O) at the beginning of 2022 should be compared with MLS observations for validation if the model participates in evaluation of the Hunga stratospheric chemistry impact.

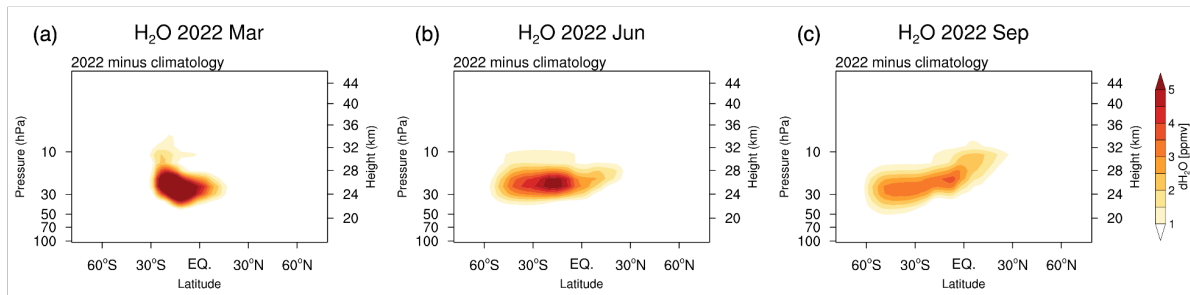
239 * 5 years is enough to reach sulfate equilibrium in the stratosphere; water may take 7 years (each model
 240 should adjust the spin-up time according to model features). ** Recommended degassing volcanic
 241 emissions injected at the cone altitude, constant flux based on Carn et al. (2017). Database is updated
 242 through 2022 here: <https://doi.org/10.5067/MEASURES/SO2/DATA406>.

243

244 **Table 2. Experiment design**

Experiment	Meteorology	period	aerosol treatment	QBO	SST	Ensemble members
Exp1_FixedSST	Free run starts Feb 1. (i.e. nudge until Jan 31)	10 years 2022-2031 (first 5 years for mesospheric analysis)	model simulated aerosol or prescribed	Internal generated (Nudge if model doesn't generate)	Fixed (climatology = mean of monthly average during the past decade (2012-2021), repeating annually) This applies to spin-up time too.	10-20
Exp1_CoupledOcean					Coupled ocean (optional) initialize with observed ocean state (see section 3 for individual model descriptions)	10-20
Exp2a	Nudged wind only and/or nudged T and wind*	2 years 2022-2023	model simulated aerosol	nudged	Observed SST	-
Exp2b	Nudged wind only and/or	2 years 2022-2023	prescribed	nudged	Observed SST	-

245
246



247
248
249
250
251

Figure 1. Monthly average water vapor perturbation after the Hunga eruption from MLS. Panels (a-c) show the observed dispersion of the H₂O enhancement in 2022 in the months of (a) March, (b) June, and (c) September.

252
253
254
255
256
257
258
259
260
261
262
263
264
265
266
267
268
269
270
271

A parallel model intercomparison project Tonga-MIP (Clyne et al., 2024) will also be part of the 2025 Hunga assessment, which is designed to explore the plume evolution between 1 day and up to 1 or 2 months after the eruption. Tonga-MIP was initiated before the APARC Hunga Activity started. It will be described in a separate paper, but we list it in this paper to document the comprehensiveness of the modeling effort for the Hunga assessment. Two purposes of Tonga-MIP cannot be achieved by Exp1 and 2: 1. The nudged experiment of Tonga-MIP aims to intercompare the microphysics processes (i.e., cloud and aerosol physics and sulfur chemistry) between different models. Therefore, all models are requested to inject 150 Tg of water, but the retaining of the water varies between models, differing from Exp1 and 2, which ask to retain ~150 Tg of water in the stratosphere. SO₂ injection is 0.5 Tg, the same as experiments in HTHHMOC. The injections are required to be injected between 25-30 km, within the latitude and longitude box of 22-14°S and 182-186°E, at a constant vertical volume mixing ratio for 6 hours starting at 4 UTC on January 15th. 2. The free-run experiment of Tonga-MIP aims to study the radiative effect of water and SO₂ on the Hunga plume descending and ascending during the first month after the eruption since the Hunga water and aerosol plumes were observed to descend several kilometers during the first monthly after the eruption (Sellito et al., 2022; Randel et al., 2024). Therefore, Tonga-MIP designed to nudge the atmosphere up until several different dates and explore the plume descending patterns with free-run atmosphere after these dates. The dates are Jan 21, Jan 26 and Jan 31. Most of the models that participate in Tonga-MIP also participate in the HTHH-MOC.

272
273

3. Model output

274
275
276
277
278
279
280
281
282

The model output covers variables based on the Chemistry-Climate Modeling Initiative (CCMI) output list with some additions specific to this study. The detailed list is provided in the **Supplementary Excel Table**. We have requested that all models generate the same variable names, units, ordering of dimensions (longitude from 0°E to 360°E; latitude from 90°S to 90°N; pressure levels from 1000 hPa to 0.03 hPa or altitude from 0 meter to 85,000 meter), and file name structure (e.g. ‘variable_domain_modelname_experimentname.nc’ or ‘domain_modelname_experimentname.variable.nc’). The examples of Experiment_name are: HTHHMOC-Exp1, HTHHMOC-Exp1and4. The example file names are:

283 Monthlymean_WACCM6MAM_HTHHMOC-Exp1-NoVolc-fixedSST.ensemble001.O3.nc or
 284 O3_Dailymean_WACCM6MAM_HTHHMOC-Exp1-H2Oonly-CoupledOcean.ensemble001.nc.

285 The 3D model output is requested on both model levels (hybrid pressure or height) and
 286 interpolated to CMIP6 plev39 grid (plev39: 1000, 925, 850, 700, 600, 500, 400, 300, 250, 200,
 287 170, 150, 130, 115, 100, 90, 80, 70, 50, 30, 20, 15, 10, 7, 5, 3, 2, 1.5, 1 0, 0.7, 0.5, 0.4, 0.3, 0.2,
 288 0.15, 0.1, 0.07, 0.05, 0.03 hPa) and for mesospheric analysis adding 0.02, 0.01, 0.007, 0.005,
 289 0.003, 0.001 above the plev39 grid.

290 Monthly mean output is requested for all variables for **Exp1** with some fields (specified
 291 in the Excel sheet) as daily mean. Some of the fields requested as daily means are specified,
 292 either as surface fields or at reduced number of pressure levels. Daily mean output is requested
 293 for all variables for **Exp2**.

294 The model output (~33 TB) of **Exp1 and Exp2** is archived at the JASMIN workspace
 295 (jasmin.ac.uk). JASMIN provides large storage space and compute facilities to facilitate the data
 296 archiving and post data analysis of this project. This reduces the need for data transfers and
 297 allows reproducible computational workflows. Seddon et al. (2023) described the facility in
 298 detail. Our next phase is to publicly release the data by transferring the data to the Centre for
 299 Environmental Data Analysis (CEDA) archiving system.

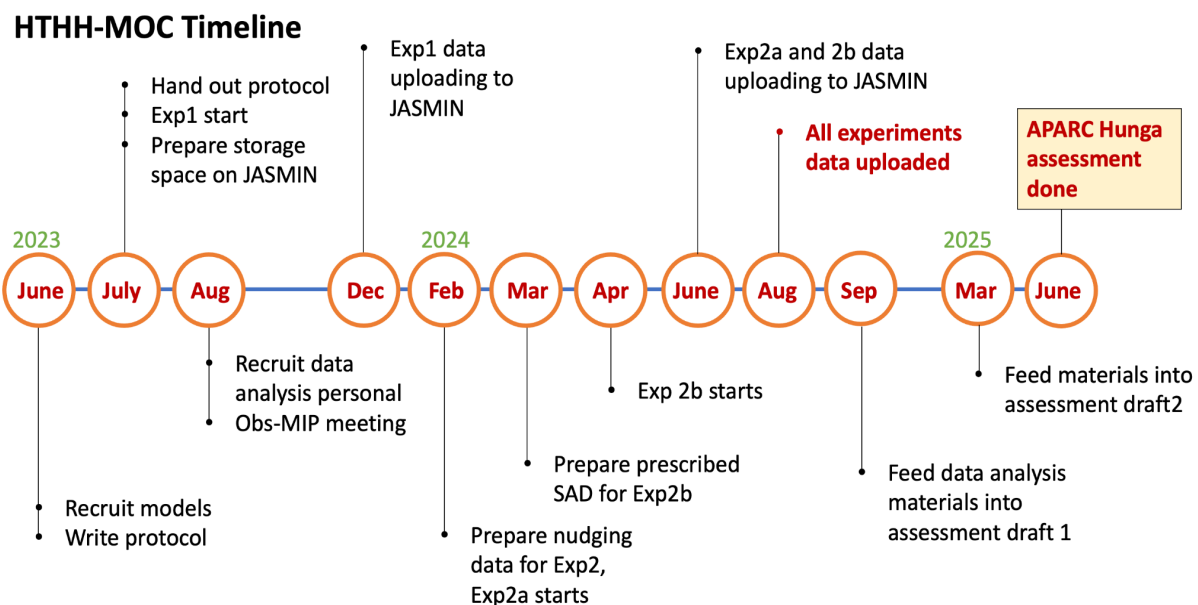
300

301 4. Model Descriptions and the Hunga Volcanic Injection Specification

302 As part of the three-year Hunga Impact activity, this project is highly time-sensitive. We
 303 designed the timeline for each experiment (**Figure 2**) to facilitate the completion of the 2025
 304 Hunga Impact assessment. However, the JASMIN workspace will remain open for the uploading
 305 of modeling data after the deadline denoted in **Figure 2** until 2025.

306 This paper only includes model descriptions for those models that submitted the output
 307 following the assessment timeline. The model setup follows the protocols listed in Section 2
 308 unless specified below. **Tables 3-6** provide key information on the participant models, which are
 309 detailed described in the following paragraphs for each model.

310



311

312 **Figure 2.** The timeline designed for HTHH-MOC in order to cooperate with the APARC HTHH
313 Impact assessment.
314

Table 3. Participating models and contact information for HTHH-MOC and Tonga-MIP.

Model name	Description reference paper	Institutions (that develop the model)	Primary contact (who runs the model)	Emails
CAM5/CARMA	Yu et al. (2015)	CU Boulder Jinan Univ.	Pengfei Yu Yifeng Peng	pengfei.yu@colorado.edu pengyfl6@lzu.edu.cn
CCSRNIES-MIROC3.2	Akiyoshi et al. (2023), Akiyoshi et al. (2016)	NIES	Yosuke Yamashita Hideharu Akiyoshi	yamashita.yosuke@nies.go.jp hakiyosi@nies.go.jp
CMAM	Jonsson et al. (2004), Scinocca et al. (2008)	CCCma, Environment and Climate Change Canada	David Plummer	david.plummer@ec.gc.ca
EMAC MPIC	Schallock et al. (2023)	MPI-C, -M, DLR	Christoph Brühl	christoph.bruehl@mpic.de
GA4 UM-UKCA	Dhomse et al. (2020)	Univ. Leeds	Graham Mann, Sandip Dhomse	G.W.Mann@leeds.ac.uk , S.S.Dhomse@leeds.ac.uk
GEOSCCM	Nielsen et al. (2017)	NASA	Peter Colarco	peter.r.colarco@nasa.gov
GEOS/CARMA	Nielsen et al. (2017)	NASA	Parker Case	parker.a.case@nasa.gov
GSFC2D	Fleming et al. (2024)	NASA	Eric Fleming	eric.l.fleming@nasa.gov
IFS-COMPO Cy49R1	Huijnen et al. (GMD, 2016), Rémy et al. (GMD, 2022)	ECMWF and team CAMS2_35	Simon Chabrilat Samuel Rémy	Simon.chabrilat@aeronomie.be sr@hygeos.com
LMDZ6.2-LR-STRATAER/LMD Z6.2-LR-STRATAER-REPROBUS	O. Boucher et al. 2020, Marchand et al., 2012	CNRS, Sorbonne Univerité, IPSL, LATMOS, LOCEAN	Marion Marchand, Slimane Bekki, Nicolas Lebas, Lola Falletti	marion.marchand@latmos.ipsl.fr , slimane.bekki@latmos.ipsl.fr , nicolas.lebas@locean.ipsl.fr , lola.falletti@latmos.ipsl.fr
MIROC-CHASER	Sekiya et al. (2016)	JAMSTEC	Shingo Watanabe, Takashi Sekiya	wnabe@jamstec.go.jp , tsekiya@jamstec.go.jp
MIROC-ES2H	Tatebe et al. (2019), Kawamiya et al. (2020)	JAMSTEC and NIES	Shingo Watanabe, Takashi Sekiya, Tatsuya Nagashima, Kengo Sudo	wnabe@jamstec.go.jp , tsekiya@jamstec.go.jp , nagashima.tatsuya@nies.go.jp , kengo@nagoya-u.jp
SOCOLv4	Sukhodolov et al. (2021)	PMOD/WRC and ETH-Zurich	Timofei Sukhodolov	timofei.sukhodolov@pmodwrc.ch
UKESM1.1	Sellar et al. (2019, 2020), with chemistry updates from Dennison et al. (2019)	UK Met Office, UK Universities and National Centre for Atmospheric Science (NCAS)	Graham Mann, Sandip Dhomse Ben Johnson Mohit Dalvi Luke Abraham James Keeble	g.w.mann@leeds.ac.uk , s.s.dhomse@leeds.ac.uk ben.johnson@metoffice.gov.uk mohit.dalvi@metoffice.gov.uk nla27@cam.ac.uk j.keeble2@lancaster.ac.uk

WACCM6/CARM A	Tilmes et al. (2023)	NCAR	Simone Tilmes Cheng-Cheng Liu Yunqian Zhu Margot Clyne (Tonga-MIP)	tilmes@ucar.edu chengcheng.liu@lasp.colorado.edu yunqian.zhu@noaa.gov margot.clyne@colorado.edu
WACCM6/MAM	Mills et al. (2016)	NCAR	Xinyue Wang Simone Tilmes Jun Zhang Wandi Yu Zhihong Zhuo Ewa Bednarz Margot Clyne (Tonga-MIP)	xinyuew@colorado.edu tilmes@ucar.edu jzhan166@ucar.edu yu44@llnl.gov zhuo.zhihong@uqam.ca ewa.bednarz@noaa.gov margot.clyne@colorado.edu

316

317

Table 4. Participating models in HTHH-MOC and Tonga-MIP.

Model names	Exp1_FixedSST	Exp1_Coupled Ocean	Exp2a	Exp2b	Tonga-MIP (clyne et al. 2024)
CAM5/CARMA			X		
CCSRNIES- MIROC3.2				X	
CMAM	X (H2O-only) (*)				
EMAC MPIC			X		
GA4 UM-UKCA					X
GEOSCCM	X		X		X
GEOS/CARMA			X		
GSFC2D	X (*)			X	
IFS-COMPO			X		
LMDZ6.2-LR- STRATAER			X		X
LMDZ6.2-LR- STRATAER- REPROBUS			X		X
MIROC- CHASER	X		X		
MIROC-ES2H					X
SOCOLv4					X
UKESM1.1			X		X
WACCM6/CAR MA			X		X
WACCM6/MA M	X(*)	X(*)	X		X

318

319

320

321

* The models that are qualified to analyze the mesospheric components are marked with * symbol.

Table 5. Model resolutions and schemes used for HTHH-MOC experiments

Model names	Horizontal resolution	nlevels	Mode l Top	Vertical resolution in the stratosphere	Aerosol scheme	Specified dynamic source	QBO for models participating free run	Chemistry package (tropospheric chemistry included?)
CAM5/CARM A	~2 deg	56	45 km	1-4 km	CARMA sectional (20 bins)	GEOS5	-	MOZART (yes)
CCSRNIES-MIROC3.2	T42	34	0.01 hPa	1-3 km	None	MERR A-2	-	full strat; no tropo
CMAM	T47	80	0.00 06 hPa	0.8 - 2.5 km	None	ERA5	nudged	stratospheric + methane-NOx in troposphere
EMAC MPIC	T63	90	0.01 hPa	0.5km in LS	GMXE, modal	ERA-5	-	MECCA, simplified troposphere
GEOSCCM	c90 (~1 deg)	72	0.01 hPa	~1 km	GOCA RT (Bulk)	MERR A-2/GEOS -FP	Internal generated	GMI (yes)
GEOS/CARMA	c90 (~1 deg)	72	0.01 hPa	~1 km	CARMA (sectional 24 bins)	MERR A-2/GEOS -FP	-	GMI (yes)
GSFC2D	4°	76	.002 hPa (~ 92 km)	1km	Prescri bed only	MERR A-2	Internal generated	full strat; partial trop
IFS-COMPO	T1511 (~40km)	137	0.01 hPa	0.5-1.5 km	Bulk	ERA5	-	BASCOE (strato) + CB05 (tropo)
LMDZ6.2-LR-STRATAER	2.5° × 1.3°	79	80k m	1-5 km	S3A(sect ional 36 bins)	ERA5	-	No
LMDZ6.2-LR-STRATAER-REPROBUS	2.5° × 1.3°	79	80k m	1-5 km	S3A(sect ional 36 bins)	ERA5	-	REPROBUS
MIROC-CHASER	T85	81	0.00 4 hPa	0.7-1.2 km	MAM 3	MERR A-2	Internal generated	troposphere-stratosphere chemistry
UKESM1.1	N96	85	80k m	0.6-0.7km in LS	GLOM AP-mode	ERA-5	Internal generated	CheST strat-trop chemistry
WACCM6/CARMA	~1 deg	70	140 km	1-2 km	Sectional (20 bins)	MERRA-2	-	MOZART (yes)
WACCM6/MAM	~1 deg	70	140 km	1-2 km	MAM4	MERRA-2	Internal generated	MOZART (yes)

322
323
324

Table 6. Hunga volcanic injection profile for HTHH-MOC experiments

Model names	Data and duration	H ₂ O amount	H ₂ O altitude	H ₂ O location/area	SO ₂ amount	SO ₂ altitude	SO ₂ location/area
-------------	-------------------	-------------------------	---------------------------	--------------------------------	------------------------	--------------------------	-------------------------------

			(left after a week)				
CAM5/CARMA	Jan 15, 6 hrs	150 Tg (~135 Tg)	25-35 km	22-14°S, 182-186°E	0.5 Tg	20-28 km	22-14°S, 182-186°E
CCSRNIES- MIROC3.2	Jan 15, instantly	150 Tg (~150 Tg)	12.0-27.6 hPa	181.4– 187.0°E, 14.0–22.3°S	-	-	-
CMAM	Feb 20, 5 days	150 Tg (~150 Tg)	near 25.5 km	zonally average	-	-	-
EMAC MPIC	Jan 16, 12hrs	136 Tg (~130 Tg)	Gaussian centered at 21.5hPa	23-19°S, 177-173°W	0.4 Tg based on obs.	23-27 km based on obs.	30°S-5°N, 90-120°W (330°)
GEOSCCM	Jan 15, 6 hrs	750 Tg (~150 Tg)	25-30 km	22-14°S, 182-186°E	0.5 Tg	25-30 km	22-14°S, 182-186°E
GEOS/CARMA	Jan 15, 6 hrs	750 Tg (~150 Tg)	25-30 km	22-14°S, 182-186°E	0.5 Tg	25-30 km	22-14°S, 182-186°E
GSFC2D	use MLS H ₂ O profile until March 1	~150 Tg (~150 Tg)	-	zonally average	-	-	-
IFS-COMPO	Jan 15, 3 hrs	190 Tg (~150 Tg)	25-30 km	400 km by 200 km centered 20°S and 175°W	0.5 Tg	25-30 km	400 km by 200 km centered 20°S and 175°W
LMDZ6.2-LR- STRATAER	Jan 15, 1 day	150 Tg (~150 Tg)	Gaussian centered at 27.5 km and standard deviation of 2.5 km	22°-14°S, 182-186°E	0.5 Tg	Gaussian centered at 27.5 km and standard deviation of 2.5 km	22-14°S, 182-186°E
LMDZ6.2-LR- STRATAER- REPROBUS	Jan 15, 1 day	150 Tg (~150 Tg)	Gaussian centered at 27.5 km and standard deviation of 2.5 km	22-14°S, 182-186°E	0.5 Tg	Gaussian centered at 27.5 km and standard deviation of 2.5 km	22-14°S, 182-186°E
MIROC-CHASER	Jan 15 4 UTC, 6 hours	186 Tg (~150 Tg)	25-30 km	22-14°S, 182-186°E	0.5 Tg	25-30 km	22-14°S, 182-186°E
UKESM1.1	Jan 15, 6 hours	150 Tg	25-30km	22-14°S 182-186°E	0.5Tg	25-30km	22-14°S, 182-186°E
WACCM6/CARMA	Jan 15, 6 hours	150 Tg (~150 Tg)	25-35km	22-6°S,182.5 -202.5°E	0.5 Tg	26.5-36 km	22-6°S,182.5 -202.5°E
WACCM6/MAM	Jan 15, 6 hours	150 Tg	25-35 km	22-14°S, 182-186°E	0.5 Tg	20-28 km	22-14°S, 182-186°E

325

326

327 4.1 CAM5/CARMA

328 The atmospheric component of the Community Atmosphere Model version 5 (CAM5)
329 (Lamarque et al., 2012) is the atmospheric component of the Community Earth System Model,
330 version 1 (CESM1.2.2, Hurrell et al., 2013), with a top at around 45 km. CAM5 has a horizontal
331 resolution of 1.9° latitude \times 2.5° longitude, utilizing the finite volume dynamical core (Lin & Rood,
332 1996). The model has 56 vertical levels, with a vertical resolution ~ 1 km in the upper troposphere
333 and lower stratosphere. The modeled winds and temperatures were nudged to the 3-hour Goddard
334 Earth Observing System 5 (GEOS-5) reanalysis data set (Molod et al., 2015) every time step (30
335 min) by 1% (i.e., a 50 h Newtonian relaxation time scale). The aerosol is interactively simulated
336 using a sectional aerosol microphysics model, the Community Aerosol and Radiation Model for
337 Atmospheres (CARMA, Yu et al., 2015). The model uses the Model for Ozone and Related
338 Chemical Tracers (MOZART) chemistry that is used for both tropospheric (Emmons et al., 2010)
339 and stratospheric chemistry (English et al., 2011; Mills et al., 2016). The volcanic emissions from
340 continuously degassing volcanoes uses the emission inventory RCP8.5 and FINNv1.5. No
341 volcanic eruptions except the Hunga 2022 eruption are included.

342 The initial volcanic injection altitude and area are determined by validating the water and
343 aerosol transportation in months shown in **Figure 1** following the tests in Zhu et al. (2022), Wang
344 et al. (2023) and Zhang et al. (2024). In these simulations, the H₂O is injected at 25 to 35 km
345 altitude and SO₂ injected at 20 to 28 km altitude. The injection latitude ranges from 22°S to 14°S,
346 and longitude ranges from 182°E to 186°E (Zhu et al., 2022). The initial injection of H₂O is 150
347 Tg, with ~ 135 Tg left after the first week following the eruption.

348

349 4.2 CCSRNIES-MIROC3.2

350 The Center for Climate System Research/National Institute for Environmental Studies -
351 Model for Interdisciplinary Research on Climate version 3.2 Chemistry Climate Model
352 (CCSRNIES-MIROC3.2 CCM) (Akiyoshi et al. 2023) was developed based on versions 3.2 of the
353 MIROC atmospheric general circulation model (AGCM), incorporating a stratospheric chemistry
354 module that was developed at National Institute for Environmental Studies (NIES) and the
355 University of Tokyo. The model has a horizontal resolution of T42 (2.8° latitude \times 2.8° longitude)
356 and 34 vertical levels, with a vertical resolution ~ 1 km in the lower stratosphere/upper troposphere
357 and ~ 3 km in the upper stratosphere and mesosphere. The top level is located at 0.01 hPa
358 (approximately 80 km).

359 The chemistry in the CCSRNIES-MIROC3.2 CCM is a stratospheric chemistry module
360 including 42 photolysis reactions, 142 gas-phase chemical reactions and 13 heterogeneous
361 reactions for multiple aerosol types (Akiyoshi et al., 2023). Tropospheric chemistry is not included,
362 but the stratospheric chemistry scheme is used for both the troposphere and mesosphere.

363 In the CCSRNIES-MIROC3.2 CCM, only **Exp2b** can be performed. The atmospheric
364 temperature and horizontal winds are nudged toward Modern-Era Retrospective analysis for
365 Research and Applications Version 2 (MERRA-2) reanalysis (Gelaro et al., 2017) with a 1-day
366 relaxation using instant values at 6-hour interval (Akiyoshi et al., 2016). The HadISST data is used
367 during the simulation.

368 The CCSRNIES-MIROC3.2 CCM does not have any microphysics scheme for volcanic
369 aerosols. The surface area and spectral optical parameters of extinction, single scattering albedo,

370 and asymmetric factor for Hunga aerosols were prescribed in the model from the GloSSAC version
371 2.22 aerosol data (Jörmann 2024). H₂O was injected instantly on 15 January 2022 at the 12 grids
372 of the model in the region 181.4°E–187.0°E in longitude, 14.0°S–22.3°S in latitude, and 12.0 hPa–
373 27.6 hPa in pressure level. A uniform number density of 1.709×10^{15} molecules/cm³ H₂O was
374 injected in each of the 12 grids which amounts to ~150 Tg.

375

376 4.3 CMAM

377 The Canadian Middle Atmosphere Model (CMAM) is based on a vertically extended
378 version of CanAM3.1, the third generation Canadian Atmospheric Model (Scinocca et al., 2008).
379 Compared to the standard configuration of CanAM3.1, for CMAM the model top was raised to
380 0.0006 hPa (approximately 95 km) and the parameterization of non-orographic gravity wave
381 drag (Scinocca, 2003) and additional radiative processes important in the middle atmosphere
382 (Fomichev et al., 2004) have been included. The gas-phase chemistry includes a comprehensive
383 description of the inorganic Ox, NO_x, HO_x, ClO_x and BrO_x families, along with CH₄, N₂O, six
384 chlorine containing halocarbons, CH₃Br and, to account for an additional 5 ppt of bromine from
385 short-lived source gases, CH₂Br₂ and CHBr₃ (Jonsson et al., 2004). A prognostic description of,
386 and associated heterogeneous chemical reactions on water ice PSCs (PSC Type II) and liquid
387 ternary solution (PSC Type Ib) particles is included, although gravitational settling
388 (dehydration/denitrification) is not calculated and species return to the gas phase when
389 conditions no longer support the existence of PSC particles.

390 The simulations for the HTHH-MOC simulations were performed at T47 spectral
391 resolution (approximately 3.8° resolution on the linear transform grid used for the model
392 physics), with 80 vertical levels giving a vertical resolution of approximately 0.8 km at 100 hPa,
393 increasing to 2.3 km above 0.1 hPa. The CMAM does not internally generate a QBO, so the
394 zonal winds in the equatorial region were nudged towards a dataset based on observed variations
395 up to December 2023, constructed using the method of Naujokat (1986) and extended into the
396 future by repeating a historical period that is congruent with the observed QBO in late 2023.
397 Water vapor from the Hunga eruption was added as a zonally average perturbation to the model
398 water over five days from 00 UTC on February 20, 2022. The spatial distribution of the anomaly
399 was designed to reproduce the water vapor anomaly observed in mid-February by the The
400 Atmospheric Chemistry Experiment - Fourier Transform Spectrometer (ACE-FTS) (Bernath et
401 al., 2005) satellite (Patrick Sheese, personal communication), with a maximum value of 13.3
402 ppm at 17°S and 25.5 km and producing an anomaly of ~150 Tg H₂O in the stratosphere.

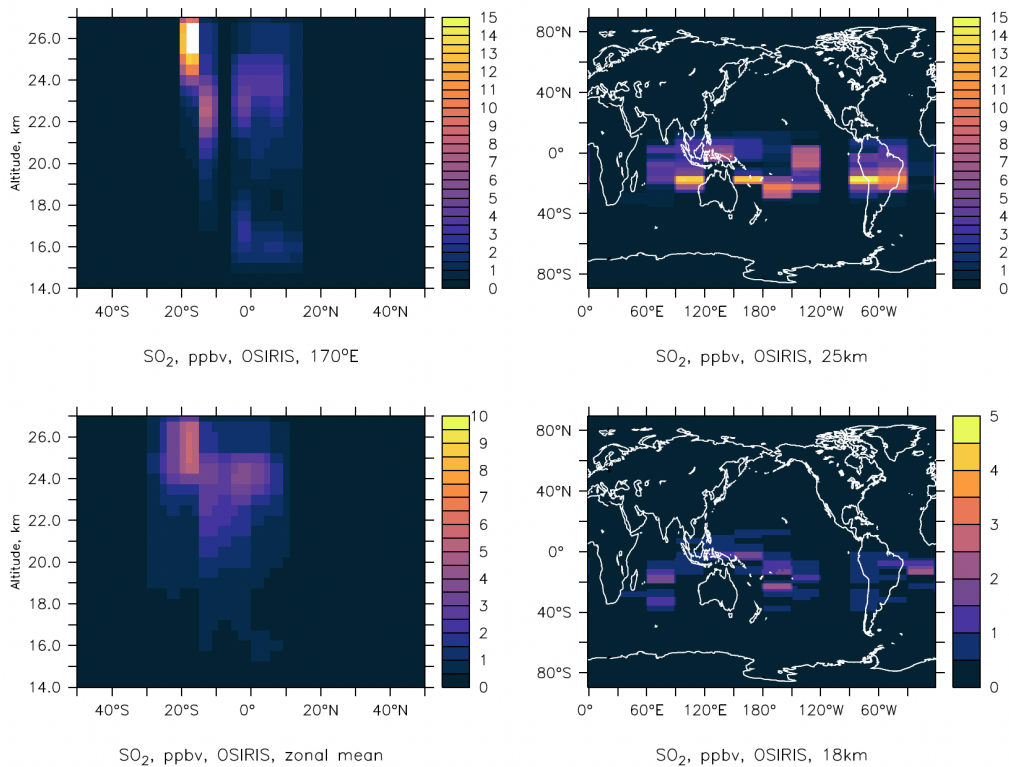
403

404 4.4 EMAC MPIC

405 The chemistry-climate model EMAC (ECHAM5/MESSy Atmospheric Chemistry)
406 consists of the European Centre Hamburg general circulation model (ECHAM5) and the
407 Modular Earth Submodel System (MESSy) (e.g., Jöckel et al., 2010). Here we use the version of
408 Schallock et al. (2023) in horizontal resolution T63 (1.87°x 1.87°) with 90 levels between the
409 surface and 0.01 hPa.

410 Vorticity, divergence, and temperatures between boundary layer and 100 hPa are nudged
411 to the ERA5 reanalysis of ECMWF (Hersbach et al., 2020), as well as surface pressure. SSTs
412 and sea ice cover are prescribed by ERA5 data. The model can generate an internal QBO but for
413 comparison with observations it was slightly nudged to the Singapore data compiled by Free
414 University of Berlin and Karlsruhe Institute of Technology.

415 The model contains gas-phase and heterogeneous chemistry on PSCs and interactive
 416 aerosols. Surface mixing ratios of chlorine- and bromine-containing halocarbons and other long-
 417 lived gases are nudged to Advanced Global Atmospheric Gases Experiment (AGAGE)
 418 observations. The microphysical modal aerosol module contains four soluble and three insoluble
 419 modes for sulfate, nitrate, dust, organic and black carbon, and aerosol water (Pringle et al.,
 420 2010). The instantaneous radiative effect by tropospheric and stratospheric aerosols can be
 421 calculated online by multiple calls of the radiation module. Volcanoes injecting material into the
 422 stratosphere are considered as in Schallock et al. (2023) using the perturbations of stratospheric
 423 SO₂ observed by the Michelson Interferometer for Passive Atmospheric Sounding (MIPAS) and
 424 aerosol extinction observed by OSIRIS. This method, based typically on data of a 10-day period,
 425 distributes the injected SO₂ over a larger volume than typical point source approaches using the
 426 same integrated mass (see also Kohl et al., 2024). For Hunga this method has the disadvantage
 427 that H₂O and SO₂ are not co-injected since H₂O is injected in 12 hours in a slab consisting of
 428 four horizontal boxes and a Gaussian vertical distribution centered at 21.5 hPa. For **Exp2a** we
 429 continue the 30-year transient simulation presented in Schallock et al. (2023) with and without
 430 Hunga Tonga. The simulated H₂O-perturbation is consistent with **Figure 1**. The SO₂ injection is
 431 derived based on the extinction from the OSIRIS observation averaged over about 10 days
 432 (**Figure 3**) (Bruehl et al., 2023).



433 **Figure 3.** The SO₂ injection used in EMAC MPIC model is based on the Hunga SO₂
 434 perturbation derived from extinction observed by OSIRIS averaged over about 10 days, i.e.,
 435 including several snapshots of the westward moving plume. For conversion from extinction to
 436 volume mixing ratio Eqn. 1 of Schallock et al (2023) is applied with $f=3$ because of data gaps.
 437 5day-averaged gridded OSIRIS data averaged from January 24 0h to February 3 0h were used.
 438 Note that the colorbars are not the same in each panel.
 439
 440

441

442 4.5 GEOSCCM

443 The NASA Goddard Earth Observing System Chemistry-Climate Model (GEOSCCM) is
444 based on the GEOS Earth system model (Reinecker et al. 2008, Molod et al. 2015). For the
445 HTHH-MOC experiments the model is run on a cubed-sphere horizontal grid at a C90 resolution
446 (~100 km) with 72 vertical hybrid-sigma levels from the surface to 0.01 hPa (~80 km).
447 Dynamics are solved using the finite-volume dynamical core (Putman and Lin, 2007). Deep and
448 shallow convection are parameterized using the Grell-Freitas (2014) and Park-Bretherton (2009)
449 schemes, respectively, and moist physics is from Bacmeister et al. (2006). The turbulence
450 parameterization is based on the non-local scheme of Lock et al. (2000). Shortwave and
451 longwave radiative fluxes are computed in 30 bands using the Rapid Radiative Transfer Model
452 for GCMs (RRTMG, Iacono et al. 2008).

453 Stratospheric and tropospheric chemistry are from the Global Modeling Initiative (GMI)
454 mechanism (Duncan et al., 2007; Strahan et al., 2007; Nielsen et al., 2017), updated here to
455 include reactions for sulfur species. The GMI mechanism in GEOSCCM has been extensively
456 evaluated for its stratospheric ozone-related photochemistry and transport in various model
457 intercomparisons, including Stratosphere-troposphere Processes and their Role in Climate
458 (SPARC) Chemistry Climate Model Validation (CCMVal), CCMVal-2, and the CCMi (SPARC-
459 CCMVal, 2010; Eyring et al., 2010, 2013; Morgenstern et al., 2017). Aerosol species are
460 simulated by the Goddard Chemistry, Aerosol, Radiation, and Transport, second generation
461 (GOCART-2G), module (Collow et al. 2024), which includes a sectional approach for dust (five
462 bins), sea salt (five bins), and nitrate (three bins), and a bulk approach for sulfate (dimethyl
463 sulfide, SO₂, methanesulfonic acid, and SO₄²⁻) aerosol and carbonaceous species (hydrophobic
464 and hydrophilic modes of “white” and “brown” organics and black carbon).

465 For the GEOSCCM simulations performed with the GOCART-2G module we use the
466 nominal GOCART-2G sulfate mechanism, updated here to use the online hydroxyl (OH) radical,
467 nitrate (NO₃) radical, and hydrogen peroxide (H₂O₂) from the GMI mechanism instead of
468 climatological fields provided from offline files (Collow et al., 2024). While not a full coupling
469 to the GMI sulfur cycle it nevertheless allows the GOCART-2G sulfate mechanism to have the
470 impact of the Hunga water vapor perturbation on the oxidants. A second “instance” of the
471 GOCART-2G sulfate mechanism is run that is specifically for the volcanic SO₂ and resultant
472 sulfate from the Hunga eruption. This allows us to track the eruptive volcanic aerosol separately
473 from the nominal sulfate instance that sees mainly tropospheric sources. We assign this volcanic
474 instance optical properties consistent with SAGE retrievals of the sulfate aerosol properties,
475 using an effective radius of 0.4 microns. We find that 750 Tg of H₂O is needed in the initial
476 injection to provide a residual ~150 Tg of water in the stratosphere after a week. All other
477 injection parameters follow the protocol. The model spinup was performed by “replaying” to the
478 MERRA-2 meteorology (Gelaro et al. 2017), and is used throughout the **Exp2a** results. A
479 MERRA-2 2012-2021 climatology of SST and sea ice fractions are used based on Reynolds et al.
480 (2002).

481

482 4.6 GEOS/CARMA

483 A second configuration of the GEOSCCM, coupled to the sectional aerosol microphysics
484 package CARMA, also simulated the eruption (GEOS/CARMA). This configuration is the same
485 as above except for the aerosol package and its coupling to the GMI chemistry mechanism. For
486 this version of GEOSCCM, we use the configuration of CARMA described in Case et al. (2023).

487 This configuration uses 24 size bins, spread logarithmically in volume between 0.25nm and
488 6.7 μ m in radius and simulates the nucleation, condensational growth, evaporation, coagulation,
489 and settling of sulfate aerosols in these simulations following the mechanism of English et al.
490 (2013). For these simulations, CARMA is fully coupled to the GMI sulfur cycle by the
491 production (i.e., oxidation of SO₂, evaporation of sulfate aerosols) and loss (i.e., nucleation and
492 condensation of sulfate aerosols) of sulfuric acid (H₂SO₄) vapor. Optical properties for the
493 CARMA aerosols are calculated based on the interactively calculated aerosol size distribution.
494 The same injection parameters for GEOSCCM described above are used by this configuration.
495 This model configuration contributed to **Exp2a** and “replayed” to MERRA-2 meteorology as
496 above.

497

498 **4.7 GSFC2D**

499 The NASA/Goddard Space Flight Center two-dimensional (2D) chemistry-climate model
500 (GSFC2D) has a domain extending from the surface to ~92 km (0.002 hPa). The model has 76
501 levels, with 1 km vertical resolution from the surface to the lower mesosphere (60 km) and 2 km
502 resolution above (60-92 km). The horizontal resolution is 4° latitude, and the model uses a 2D
503 (latitude-altitude) finite volume dynamical core (Lin & Rood, 1996) for advective transport. The
504 model has detailed stratospheric chemistry and reduced tropospheric chemistry, with a diurnal
505 cycle computed for all constituents each day (Fleming et al., 2024). The model uses prescribed
506 zonal mean surface temperature as a function of latitude and season based on a multi-year
507 average of MERRA-2 data (Gelaro et al., 2017). Zonal mean latent heating, tropospheric water
508 vapor, and cloud radiative properties as a function of latitude, altitude, and season are also
509 prescribed (Fleming et al., 2020).

510 For the free-running simulations, the model planetary wave parameterization (Bacmeister
511 et al., 1995; Fleming et al., 2024) uses lower boundary conditions (750 hPa, ~2 km) of
512 geopotential height amplitude and phase for zonal wave numbers 1–4. These are derived as a
513 function of latitude and season using: 1) a 30-year average (1991–2020) of MERRA-2 data for
514 the standard yearly-repeating climatological-dynamics simulations (“Clim-NoQBO”); and 2)
515 individual years of MERRA-2 data (1980-2020) randomly rearranged in time to generate
516 interannual variations in stratospheric dynamics (“ensemble1”, “ensemble2”,...“ensemble10”).
517 For the inter-annually varying dynamics simulations, the model includes an internally generated
518 QBO (Fleming et al., 2024).

519 For experiments that include the Hunga volcanic aerosols, the simulations go through the
520 end of 2023, using prescribed aerosol properties for 2022-2023 from both the GloSSAC data set
521 and derived from the OMPS-LP data (Taha et al., 2021, 2022). For experiments that include the
522 Hunga H₂O injection, Aura/MLS observations are used to derive a daily zonal mean Hunga
523 water vapor anomaly in latitude-altitude, which is added to the baseline H₂O (no volcano)
524 through the end of February 2022. This combined water vapor field is then fully model computed
525 starting 1 March 2022 through the end of 2031.

526 For **Exp2b**, the model zonal mean temperature and transport fields are computed from
527 the MERRA-2 reanalysis data. These are input into the model and used as prescribed fields (no
528 nudging is done).

529

530 **4.8 IFS-COMPO**

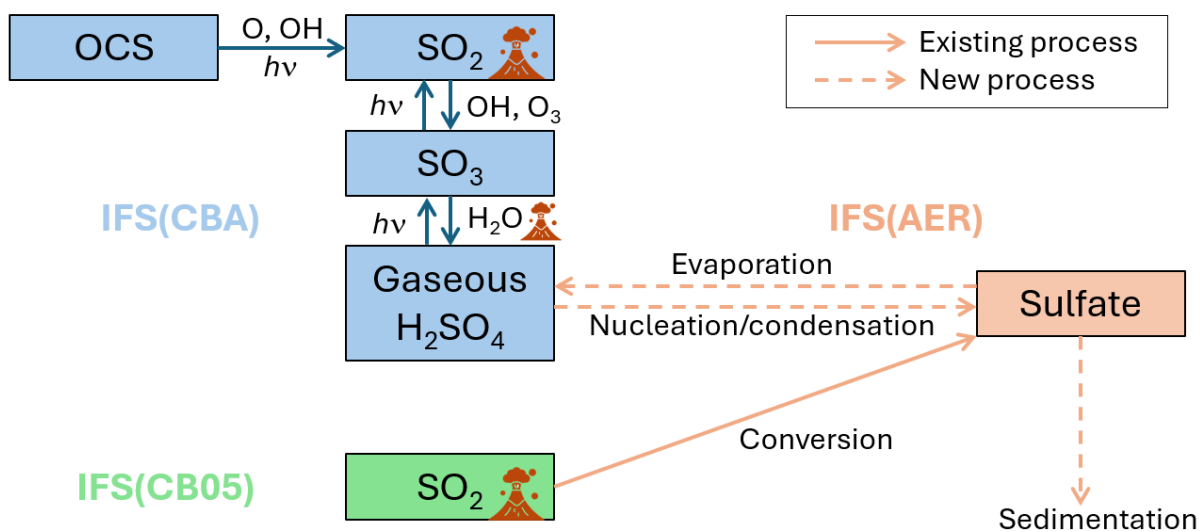
531 The Copernicus Atmosphere Monitoring Service (CAMS) provides daily global analysis
532 and 5-day forecasts of atmospheric composition (aerosols, trace gases, and GHGs) (Peuch et al.

533 2022). CAMS is coordinated by the European Centre for Medium Range Weather Forecasts
 534 (ECMWF) and uses, for its global component, the Integrated Forecasting System (IFS), with
 535 extensions to represent aerosols, trace, and GHGs, being called "IFS-COMPO" (also previously
 536 known as "C-IFS", Flemming et al. 2015). IFS-COMPO is composed of IFS(AER) for aerosols,
 537 as described in Remy et al. (2022) while the atmospheric chemistry is based on the chemistry
 538 module as described in Williams et al. (2022) for the troposphere (IFS-CB05) and Huijnen et al.
 539 (2016) for the stratosphere (IFS-CBA). The stratospheric chemistry module of IFS-COMPO is
 540 derived from the Belgian Assimilation System for Chemical ObErvations (BASCOE, Errera et al
 541 2019). IFS-COMPO stratospheric chemistry is used since the operational implementation of cycle
 542 48R1 on June 27, 2023 (Eskes et al., 2024).

543 The aerosol component of IFS-COMPO is a bulk aerosol scheme for all species except sea
 544 salt aerosol and desert dust, for which a sectional approach is preferred, with three bins for each
 545 of these two species. Since the implementation of operational cycle 48R1 in June 2023, the
 546 prognostic species are sea salt, desert dust, organic matter (OM), black carbon (BC), sulfate, nitrate,
 547 ammonium, and secondary organic aerosols (SOA).

548 For **Exp2a**, cycle 49R1 IFS-COMPO has been used, which will become operational for
 549 CAMS production in November 2024, at a resolution of TL511 (~40 km grid cell) over 137 model
 550 levels from surface to 0.01 hPa. Cycle 49R1 IFS-COMPO integrates a number of updates of
 551 tropospheric and stratospheric aerosols and chemistry. The most relevant aspect for this work
 552 concerns the representation of stratospheric aerosols, which has been revisited with the
 553 implementation of a coupling to the stratospheric chemistry through a simplified stratospheric
 554 sulfur cycle including nucleation/condensation and evaporation processes, as shown in **Figure 4**.
 555 Direct injection of water vapor into the stratosphere is expected to enhance the nucleation and
 556 condensation of sulfate through the reaction with SO₃ and production of gas-phase H₂SO₄.

557 The volcanic injection takes place between 3 and 6 UTC on January 15, 2022, with a
 558 uniform vertical distribution between 25 and 30 km of altitude, over a rectangular region of 400
 559 km (latitude) x 200 km (longitude) centered on the coordinates of the Hunga volcano. The injected
 560 quantities are 0.5 Tg SO₂ and 190 Tg H₂O.
 561



562
 563 **Figure 4.** Architecture of the stratospheric extension of IFS(AER) and its coupling with IFS(CBA)
 564 and IFS(CB05), with existing and new processes implemented in cycle 49R1 of IFS-COMPO. *hν*

565 represents photolysis and the volcano symbols represent direct injections by volcanic eruptions.
566 Sedimentation is indicated as a new process because it has been revisited.

567
568

569 **4.9 LMDZ6.2-LR-STRATAER and LMDZ6.2-LR-STRATAER-REPROBUS**

570 The Institut Pierre-Simon Laplace Climate Modelling Centre (IPSL CMC, see
571 <https://cmc.ipsl.fr>) has set up a new version of its climate model in the runup of CMIP6. Further
572 description of the IPSL-CM6A-LR climate model can be found in Boucher et al. (2020) and in
573 Lurton et al. (2020). New development of the model is now ongoing to prepare the IPSLCM7
574 version.

575 The IPSLCM7 climate model is using the general circulation model named LMDZ for
576 *Laboratoire de Météorologie Dynamique-Zoom* (Hourdin et al., 2006). The LMDZ version used
577 for this study is based on a regular horizontal grid with 144 points regularly spaced in longitude
578 and 142 in latitude, corresponding to a resolution of $2.5^\circ \times 1.3^\circ$. The model has 79 vertical layers
579 and extends up to 80 km, which makes it a “high-top” model. The model shows a self-generated
580 quasi-biennial oscillation (QBO) whose period has been tuned to the observed one for the
581 present-day climate (Boucher et al., 2020).

582 The aerosol is interactively simulated in the STRATAER module using a sectional
583 scheme with 36 size bins. STRATAER is an improved version of the Sectional Stratospheric
584 Sulfate Aerosol (S3A) module (Kleinschmitt et al., 2017). It now takes into account the
585 photolytic conversion of H_2SO_4 into SO_2 in the upper stratosphere (Mills et al., 2005). The size-
586 dependent composition of $\text{H}_2\text{SO}_4/\text{H}_2\text{O}$ aerosols is now computed iteratively to ensure that the
587 surface tension, density, and composition are consistent in the calculation of the Kelvin effect.
588 The surface tension, density, H_2SO_4 vapor pressure, and nucleation rates are calculated based on
589 Vehkamäki et al. (2002). The version of the LMDZ6.2-LR-STRATAER atmospheric model used
590 in the HTHH Impact project accounts for the stratospheric H_2O source from methane oxidation.
591 The chemistry is simulated using the REPROBUS (*REactive Processes Ruling the Ozone*
592 *BUDget in the Stratosphere*) chemistry module that includes 55 chemical species and a
593 comprehensive description of the stratospheric chemistry (Marchand et al., 2012, Lefèvre et al.,
594 1994, Lefèvre et al., 1998).

595 For **Exp2a**, the H_2O and SO_2 is injected at 27.5 km altitude using a Gaussian distribution
596 and standard deviation of 2.5 km. The injection latitude ranges from 22°S to 14°S , and longitude
597 ranges from 182°E to 186°E . The injections of H_2O and SO_2 are 150 Tg and 0.5 Tg, respectively.
598 The SSTs are taken from the IPSL climate coupled simulation run under the CMIP6 Tier 1
599 SSP2-4.5 scenario (Neil et al., 2016).

600

601 **4.10 MIROC-CHASER**

602 The Model for Interdisciplinary Research On Climate - CHEMical Atmospheric general
603 circulation model for Study of atmospheric Environment and Radiative forcing (MIROC-
604 CHASER) version 6 (Sekiya et al. 2016) is a chemistry climate model, with a top at around 0.004
605 hPa. The present version of MIROC-CHASER is built on MIROC6 (Tatebe et al. 2019) and has a
606 spectral horizontal resolution of T85 (1.4° latitude \times 1.4° longitude). The model has 81 vertical
607 levels, with a vertical resolution 0.7 km in the lower stratosphere, ~ 1.2 km in the upper stratosphere,
608 and ~ 3 km in the lower mesosphere. In the free-running simulations, the model generates
609 QBO internally. The ensemble members have different initial conditions (January 1, 2022), which
610 are generated using slightly different nudging relaxation time during the spin-up. The aerosols are

611 interactively simulated using a three-mode modal aerosol module (Seikiya et al. 2016). The
612 chemistry uses comprehensive troposphere-stratosphere chemistry (Watanabe et al. 2011). The
613 volcanic emission from continuously degassing volcanoes uses the emission inventory of Fioletov
614 et al. (2022). For the explosive volcanic eruptions during the spin-up time, explosive volcanic
615 emissions follow Carn (2022).

616 For **Exp1** fixed SST simulations, the model uses the observed SST from 10-year
617 climatological mean from 2012 to 2021 using the monthly-1deg CMIP6 AMIP SST (Gates et al.,
618 1999).

619 For **Exp2a**, the atmospheric temperature and winds are nudged to MERRA-2 reanalysis
620 with a 12-hour relaxation using 3-hour meteorology. The observed SST uses the NOAA 1/4° Daily
621 Optimum Interpolation Sea Surface Temperature (OISST) from 2022 to 2023 (Huang et al. 2020).

622 The initial volcanic injection altitude and area are not tuned but follow the experimental
623 protocol. For **Exp1** and **Exp2a**, the H₂O and SO₂ are injected at 25 to 30 km altitude. The injection
624 latitude ranges from 22°S to 14°S, and longitude ranges from 182°E to 186°E. The initial injection
625 of H₂O is 186 Tg, with ~150 Tg left after the first week following the eruption. The large initial
626 H₂O injection is necessary to keep 150 Tg in the stratosphere as requested by the experimental
627 protocol, because a large amount of ice clouds generates and falls to the troposphere soon after the
628 eruption.

629

630 4.11 UKESM1.1

631 The United Kingdom Earth System Model (UKESM, Sellar et al., 2019, 2020) is the
632 successor to the HadGEM2-ES model (Collins et al., 2011), jointly developed by the UK Met
633 Office and the Natural Environment Research Council (NERC) to deliver simulations to the
634 Coupled Model Intercomparison Project Phase 6 (CMIP6; Eyring et al., 2016). For HTHH-MOC,
635 we run the updated UKESM1.1 system (Mulcahy et al., 2023) which consists of the physical
636 climate model HadGEM3-GC3.1 (Kuhlbrodt et al., 2018; Williams et al., 2018), and has improved
637 tropospheric aerosol processes and aerosol radiative forcings (Mulcahy et al., 2018; 2020). The
638 GC3.1 system comprises the GA7.1 global atmosphere model configuration (Walters et al., 2019),
639 which uses the ENDGAME dynamics system (Wood et al., 2014), at a resolution of 1.875°
640 longitude by 1.25° latitude with 85 levels extending to 85 km. Specifically the simulations apply
641 the UKESM1.1-AMIP academic community release job (at v12.1 of the Unified Model), as
642 supported by the UK National Centre for Atmospheric Science.

643 The interactive atmospheric chemistry module UKCA (UK Chemistry and Aerosols) has a
644 number of chemistry configurations; with UKESM1.0 for CMIP6 applying the combined
645 stratosphere and troposphere chemistry (CheST) option (Archibald et al., 2020), essentially a
646 combination of the stratosphere chemistry (Morgenstern et al., 2009) and tropospheric chemistry
647 (O'Connor et al., 2014) UKCA schemes. The UKCA aerosol scheme is the GLOMAP-mode
648 aerosol microphysics module (Mann et al., 2010; 2012; Bellouin et al., 2013), with UKESM1.0
649 including the initial set of adaptations to GLOMAP for simulating stratospheric aerosol (Dhomse
650 et al., 2014). For all UKESM1.0 integrations for CMIP6, the system was applied with evaporation
651 of sulphate aerosol de-activated, stratospheric aerosol properties enacted from the CMIP6
652 prescribed zonal mean data set (Luo, 2017), but for the integrations here we have applied the
653 system for interactive aerosol across the troposphere and stratosphere, enacting a Hunga emission
654 of volcanic SO₂ following the 0.5Tg@25-30km Tonga-MIP protocols (see **Table 6**).

655 For the improved UKESM1.1 version applied here, the other most relevant development,
656 compared to UKESM1.0 used for CMIP6, is the interactive atmospheric chemistry module UKCA

657 (UK Chemistry and Aerosols) has the updates to heterogeneous chemistry added by Dennison et
658 al. (2019), to represent more realistically reactions occurring on the surfaces of polar stratospheric
659 clouds and sulfate aerosol, with modified uptake coefficients of the five existing reactions and the
660 addition of a further eight reactions involving bromine species. For these simulations, we have
661 added to UKESM for the first time the equilibrium liquid PSC scheme of Carslaw et al. (1995), an
662 interim implementation here coupling the 5 existing heterogeneous reactions chlorine activation
663 then occurring on both solid and now also liquid ternary-aerosol PSCs.

664 For **Exp2**, UKESM1.1 is run in specified dynamics configuration (Telford et al., 2008,
665 2009), the atmospheric temperature and winds nudged to ERA5 every 6 hours, the Newton
666 relaxation applied for levels 12 to 80 of 85 (between 1 km and 60 km) Sea-surface temperatures
667 and sea-ice are prescribed from the Reynolds v2.1 datasets, both during the 2017 to 2022 spin-up
668 period, and the 2-year experiment 2 period to December 2023. Monthly varying anthropogenic
669 atmospheric chemistry and aerosol emissions were set following the CMIP6 SSP2-4.5 datasets.

670
671

672 **4.12 WACCM6/MAM4**

673 The Whole Atmosphere Community Climate Model version 6 (WACCM6; Gettelman et
674 al. 2019) is the high-top version of the atmospheric component of the Community Earth System
675 Model, version 2 (CESM2), with a top at around 140 km. WACCM6 has a horizontal resolution
676 of 0.9° latitude \times 1.25° longitude, utilizing the finite volume dynamical core (Lin & Rood,
677 1996). The model has 70 vertical levels, with a vertical resolution \sim 1 km in the lower
678 stratosphere, \sim 1.75 km in the upper stratosphere, and \sim 3.5 km in the upper mesosphere and lower
679 thermosphere (Garcia et al., 2017). In the free-running simulations, the model generates QBO
680 internally (Mills et al., 2017; Gettelman et al. 2019). The ensemble members differ in the last
681 date of nudging (from January 27 to February 5, 2022). The aerosol is interactively simulated
682 using a four-mode modal aerosol module (MAM4; Liu et al., 2012, 2016; Mills et al., 2016), in
683 which we used the Vehkamäki nucleation scheme (Vehkamäki et al., 2002). The chemistry uses
684 comprehensive troposphere-stratosphere-mesosphere-lower-thermosphere (TSMLT) chemistry
685 (Gettelman et al. 2019). The volcanic emissions from continuously degassing volcanoes use the
686 emission inventory of Andres and Kasgnoc (1998). For the explosive volcanic eruptions during
687 the spin-up time, explosive volcanic emissions follow Mills et al. (2016) and Neely III and
688 Schmidt (2016) with updates until 2022.

689 For **Exp1_CoupledOcean** simulations, the ocean and sea-ice are initialized on January
690 3, 2022 with output from a standalone ocean model forced by atmospheric state fields and fluxes
691 from the Japanese 55-year Reanalysis (Tsujino et al., 2018). To accurately simulate the early
692 plume structure and evolution, the winds and temperatures in WACCM are nudged toward the
693 Analysis for Research and Applications, MERRA-2 meteorological data (Gelaro et al., 2017)
694 throughout January 2022. After February 1, 2022, the model is free-running to capture fully-
695 coupled variability. For the fixed SST simulation, the model uses the 10-year climatology SST
696 from 2012 to 2021. The SST data is OISSTv2, which is a NOAA High-resolution (0.25×0.25)
697 Blended Analysis of Daily SST and Ice (Banzon et al., 2022).

698 For **Exp2**, the atmospheric temperature and winds are nudged to MERRA-2 reanalysis
699 with a 12-hour relaxation using 3-hour meteorology (Davis et al., 2022). The observed SST uses
700 10-year climatological mean from 2012 to 2021.

701 The initial volcanic injection altitude and area are the same as described for section 4.1
702 CAM5/CARMA.

703

704 **4.13 WACCM6/CARMA**

705 WACCM6/CARMA only performed **Exp2** and used a configuration similar to
706 WACCM6/MAM4 with the same horizontal and vertical resolution, SSTs, and meteorological
707 nudging. Differences compared to WACCM6/MAM4 are the chemistry and aerosol
708 configuration used. WACCM6/CARMA used the middle atmosphere chemistry with limited
709 chemistry in the troposphere and comprehensive chemistry in the stratosphere, mesosphere and
710 lower thermosphere (Davis et al., 2022). Furthermore, we use the Community Aerosol and
711 Radiation Model for Atmospheres (CARMA, Tilmes et al. 2023, based on Yu et al., 2015 with
712 some updates) as the aerosol module, in which we used the Vehkamäki nucleation scheme
713 (Vehkamäki et al., 2002). CARMA defines 20 mass bins and tracks the dry mass of the particles
714 and assumes particle water is in equilibrium with the environmental water vapor. The
715 approximate radius ranges from 0.2 nm to 1.3 μm in radius for the pure sulfate group that sulfate
716 homogeneous nucleation occurs in, and ranges from 0.05 to 8.7 μm in the mixed group that
717 tracks all major tropospheric aerosol types (i.e. black carbon, organic carbon, sea salt, dust,
718 sulfate).

719 The initial volcanic injection altitude and area are determined by validating the water and
720 aerosol transportation in the first six months against MLS and OMPS observations. In these
721 simulations, the H_2O is injected to 25 to 35 km altitude following Zhu et al. (2022), while the SO_2
722 is injected 82% of the total mass to 26.5-28 km and 18% to 28-36 km altitude. The injection latitude
723 ranges from 22°S to 6°S, and longitude ranges from 182.5°E to 202.5°E.

724

725 **5. Preliminary results**

726 The models' performances will be evaluated focusing on the following aspects: the
 727 stratospheric aerosol optical depth will be compared with GloSSAC and other satellite instruments
 728 individually such as OMPS-LP, SAGEIII-ISS, and OSIRIS; the aerosol effective radius will be
 729 compared with balloon observations (Asher et al., 2024), SAGEIII-ISS retrieved size distribution
 730 and AeroNet retrieved particle radius; the water vapor lifetime, ozone and its related chemicals
 731 (such as HCl, HNO₃, ClO) will be compared with MLS observations; the temperature anomaly
 732 will be compared with MLS detrended temperature field (Randel et al., 2024). All the evaluations

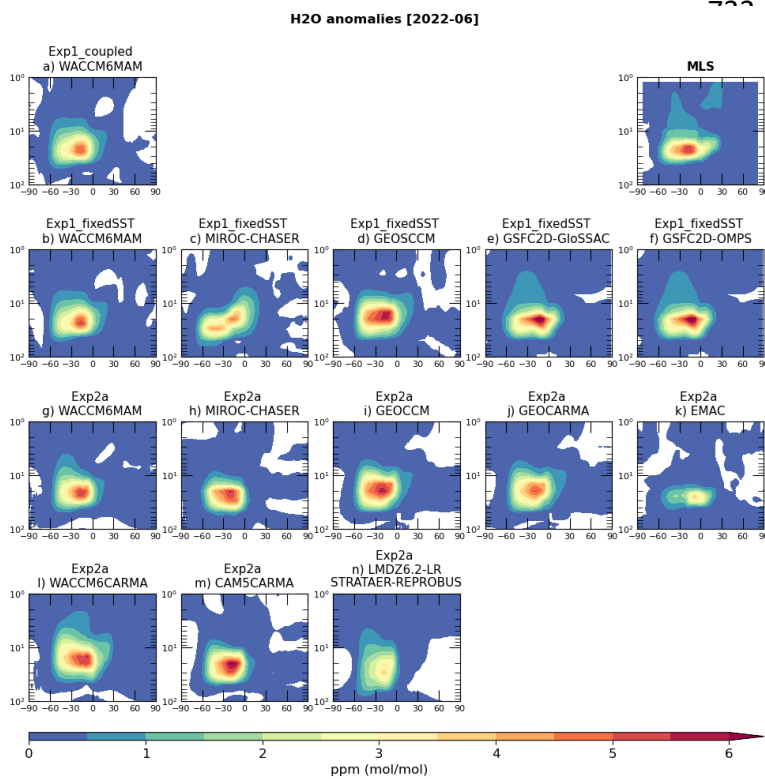


Figure 5. the zonal average H₂O anomaly in June 2022 from MLS, Exp1_fixedSST, Exp1_CoupledOcean and Exp2a. The simulated anomaly is using H₂O+SO₂ run minus the control run. And the MLS uses the 2022 data minus the climatology.

will be conducted before looking into the climate impact of this eruption, such as radiative impact and tropospheric responses. This work will be described in a follow up manuscript.

As this manuscript is written, we are still completing the model output inspection and validation phase. So, we can only provide preliminary results from some models. **Figure 5** shows the preliminary results from Exp1 and Exp2 in June 2022 compared with the MLS v5 water vapor anomaly. The model results shown here generally agree with MLS anomaly regarding the vertical (10-50 hPa) and horizontal distribution (60°S to 20°N), and the anomaly peaking at ~ 6 ppmv for most of the models. This consistency of water vapor anomaly six months after the eruption helps us have

760 confidence in these models on the analysis of climate and chemistry impacts, and will be evaluated
 761 in detail in the follow up studies.

762
 763 **6. Summary**

764 A multi-model observation comparison project is designed to evaluate the impact of the
 765 2022 Hunga eruption. Two experiments are designed to cover various research interests for this
 766 eruption, including sulfate and water plume dispersion and transport, dynamical and chemical
 767 responses in the stratosphere, and climate impact. The project will not only benefit the Hunga
 768 Impact assessment, but also benchmark the model performance on simulating stratospheric
 769 explosive volcanic eruption events and stratospheric water vapor injections. These events have a

770 potentially large impact on the Earth system, especially on the stratospheric ozone layer and
771 radiative balance.

772
773

774 **Code/Data availability**

775

776 The data used to produce the results used in this paper is archived on Zenodo: Wang, X. (2025).
777 MLS H2O anomaly 2022 [Data set]. Zenodo. <https://doi.org/10.5281/zenodo.14962954>; Quaglia,
778 I., Aquila, V., & Zhuo, Z. (2025). HTHHMOC zonal average H2O anomaly in June 2022 from
779 multi-model data [Data set]. Zenodo. <https://doi.org/10.5281/zenodo.14963276>; Andrin, J.
780 (2025). REMAP-GloSSAC-2023 [Data set]. Zenodo. <https://doi.org/10.5281/zenodo.14961868>;
781 Brühl, C. (2025). SO2 emission for EMAC MPIC model [Data set]. Zenodo.
782 <https://doi.org/10.5281/zenodo.14962925>.

783

784 **Author Contributions:**

785 Y.Z. Concept design, Project Administration, Experiment design, data archive, WACCM models
786 setup;

787 E.A. provides NOAA balloon aerosol and water vapor observations for experiments

788 E.B. and S.T. and J.Z. Experiment design, conducts experiments using WACCM6MAM;

789 A.B. Experiment design, Data archive;

790 A.J. Experiment 2b prescribed fields preparation;

791 M.K. provides GloSSAC data for Exp 2b;

792 Takashi S. and S.W.: S.W. conducted all MIROC-CHASER experiments, data post-processing,
793 data archive under supervision of Takashi S., who developed the aerosol microphysics scheme of
794 the model.

795 X.W. and W.Y. Conducts experiment using WACCM6MAM;

796 Z.Z. Conducts experiment using WACCM6MAM, WACCM6MAM data post-processing, data
797 archive;

798 N.L. and S.B.: Conducts experiment using IPSL7-STRATAER, data post-processing and archive

799 M.M. and L.F.: Conducts experiment using IPSL7-STRATAER-REPROBUS, data post-
800 processing and archive

801 S.R. and S.C. Conducts experiments using IFS-COMPO

802 M.C. Experiment design, Tonga-MIP lead;

803 F.F.Ø., G.K., O.M. contributed to experiment design

804 C.B. Conducts experiment using EMAC

805 I.Q., V.A., R.U. and A.K. Model output inspection and evaluation

806 E.F. Conducts experiments using GSFC2D, data post-processing, and data archive.

807 D.P. Contributed to experiment design and conducted experiments using CMAM and data post-
808 processing

809 P.R.C., L.D.O., Q.L., M.M., and S.S. Contributed to experiment design and conducted
810 experiments with the NASA GEOS CCM

811 P.C. and P.R.C. Contributed to experiment design and conducted experiments with the NASA
812 GEOS CARMA model

813 H.A. and Y.Y. Conducts experiment using CCSRNIES-MIROC3.2, data post-processing and
814 archive

815 D.V. contributed to experiment design and assisted E.B. with variables request

816 W.R. and P.N. concept design

817 G.M. concept design and in charge of JASMIN data archiving
818 P.Y. and Y.P. conduct experiments using CAM5CARMA and data post-processing
819 S.T. and C.-C. L. conduct experiments using WACCM6CARMA and data post-processing
820

821 **Competing interests**

822 We declare at least one of the co-authors is on the editorial board of GMD.
823

824 **Acknowledgement:**

825 We acknowledge Michelle Santee, Martyn Chipperfield, Allegra Legrande, Thomas Peter,
826 Myriam Khodri for their valuable input for this project.

827 We acknowledge the APARC for their funding and other support on this activity.

828 This research has been supported by the National Oceanic and Atmospheric Administration
829 (grant nos. 03- 01-07-001, NA17OAR4320101, and NA22OAR4320151). NCAR's Community
830 Earth System Model project is supported by the National Center for Atmospheric Research,
831 which is a major facility sponsored by the NSF under Cooperative Agreement No. 1852977.

832 W.Y.'s work was performed under the auspices of the U.S. Department of Energy by Lawrence
833 Livermore National Laboratory under Contract DE-AC52-07NA27344. TS and SW were
834 supported by MEXT-Program for the advanced studies of climate change projection (SENTAN)
835 Grant Number JPMXD0722681344 and their MIROC-CHASER and MIROC-ES2H simulations
836 were conducted using the Earth Simulator at JAMSTEC. IFS-Compo is supported by the
837 Copernicus Atmosphere Monitoring Service (CAMS), which is one of six services that form
838 Copernicus, the European Union's Earth observation programme.

839 The IPSLCM7 model experiments were performed using the high-performance computing
840 (HPC) resources of TGCC (Très Grand Centre de Calcul) under allocations 2024-A0170102201
841 (project gen2201) provided by GENCI (Grand Équipement National de Calcul Intensif). This
842 study benefited from the ESPRI (Ensemble de Services Pour la Recherche l'IPSL) computing
843 and data centre (<https://mesocentre.ipsl.fr>) which is supported by CNRS, Sorbonne Université,
844 École Polytechnique and CNES.

845 V.A. is supported by the NASA NNH22ZDA001N-ACMAP and NNH19ZDA001N-IDS
846 programs.

847 F.F.Ø. acknowledge support from the European Union's Horizon 2020 research and innovation
848 programme under the Marie Skłodowska-Curie grant 891186.

849 R.U. is supported by NASA Upper Atmospheric Composition Observations and Aura Science
850 Team programs as well as through the NASA Internal Scientist Funding Model.

851 P.R.C., L.D.O., Q.L., S.S., M.M., and P.C. are supported by the NASA Modeling Analysis and
852 Prediction program (program manager: David Considine, NASA HQ) through the NASA
853 Internal Scientist Funding Model. P.C. is additionally supported by the NASA Postdoctoral
854 Program. GEOS CCM and GEOS CARMA simulations were performed at the NASA Center for
855 Climate Simulation.

856 H.A. and Y.Y were supported by KAKENHI (JP24K00700 and JP24H00751) of the Ministry of
857 Education, Culture, Sports, Science, and Technology, Japan, and NEC SX-AURORA
858 TSUBASA at NIES were used to perform CCSRNIES-MIROC3.2 simulations.

859 GC acknowledges funding from the European Commission via the ERC StG 101078127 and the
860 Spanish Ministry of Science and Innovation via the Ramon y Cajal grant no. RYC2021-033422-
861 I.

862 We acknowledge funding from the UK National Centre for Atmospheric Science (NCAS)
863 for Graham Mann and Sandip Dhomse via the NERC multi-centre Long-Term Science
864 programme on the North Atlantic climate system (ACSYS, NERC grant NE/N018001/1.
865

866
867

References:

- 868 Akiyoshi, H., M. Kadowaki, Y. Yamashita, T. Nagatomo (2023), Dependence of column ozone
869 on future ODSs and GHGs in the variability of 500-ensemble members. *Sci. Rep.* 13,
870 320(1–12). <https://doi.org/10.1038/s41598-023-27635-y>
- 871 Akiyoshi, H., T. Nakamura, T. Miyasaka, M. Shiotani, and M. Suzuki (2016), A nudged
872 chemistry-climate model simulation of chemical constituent distribution at northern high-
873 latitude stratosphere observed by SMILES and MLS during the 2009/2010 stratospheric
874 sudden warming, *J. Geophys. Res. Atmos.*, 121, 1361-1380, doi:10.1002/2015JD023334
- 875 Andres, R. J., and A. D. Kasgnoc (1998), A time-averaged inventory of subaerial volcanic sulfur
876 emissions, *J. Geophys. Res.*, 103(D19), 25,251–25,261, doi:10.1029/98JD02091.
- 877 Archibald, A. T., O'Connor, F. M., Abraham, N. L., Archer-Nicholls, S., Chipperfield, M. et al.:
878 Description and evaluation of the UKCA stratosphere–troposphere chemistry scheme
879 (StratTrop v1.0) implemented in UKESM1, *Geosci. Model Dev.*, 13, 1223–1266,
880 <https://doi.org/10.5194/gmd-13-1223-2020>, 2020
- 881 Bacmeister, J. T., Schoeberl, M. R., Summers, M. E., Rosenfield, J. E., & Zhu, X. (1995).
882 Descent of long-lived trace gases in the winter polar vortex. *Journal of Geophysical*
883 *Research*, 100(D6), 11669–11684. <https://doi.org/10.1029/94jd02958>
- 884 Bacmeister, J. T., Suarez, M. J., & Robertson, F. R. (2006). Rain reevaporation, boundary layer–
885 convection interactions, and Pacific rainfall patterns in an AGCM. *Journal of the*
886 *Atmospheric Sciences*, 63(12), 3383-3403.
- 887 Banzon, Viva &, Reynolds, Richard & National Center for Atmospheric Research Staff (Eds).
888 Last modified 2022-09-09 "The Climate Data Guide: SST data: NOAA High-resolution
889 (0.25x0.25) Blended Analysis of Daily SST and Ice, OISSTv2." Retrieved
890 from [https://climatedataguide.ucar.edu/climate-data/sst-data-noaa-high-resolution-](https://climatedataguide.ucar.edu/climate-data/sst-data-noaa-high-resolution-025x025-blended-analysis-daily-sst-and-ice-oisstv2)
891 [025x025-blended-analysis-daily-sst-and-ice-oisstv2](https://climatedataguide.ucar.edu/climate-data/sst-data-noaa-high-resolution-025x025-blended-analysis-daily-sst-and-ice-oisstv2) on 2025-02-04.
- 892 Bellouin, N., Mann, G. W., Woodhouse, M. T., Johnson, C. E., Carslaw, K. S. and Dalvi, M.
893 Impact of the modal aerosol scheme GLOMAP-mode on aerosol forcing in the Hadley
894 Centre Global Environmental Model, *Atmos. Chem. Phys.*, 13, 3027–3044,
895 <https://doi.org/10.5194/acp-13-3027-2013>, 2013.
- 896 Bernath, P. F., McElroy, C. T., Abrams, M. C., Boone, C. D., Butler, M., Camy-Peyret, C.,
897 Carleer, M., Clerbaux, C., Coheur, P.-F., Colin, R., DeCola, P., DeMazière, M.,
898 Drummond, J. R., Dufour, D., Evans, W. F. J., Fast, H., Fussen, D., Gilbert, K., Jennings,
899 D. E., Llewellyn, E. J., Lowe, R. P., Mahieu, E., McConnell, J. C., McHugh, M., McLeod,
900 S. D., Michaud, R., Midwinter, C., Nassar, R., Nichitiu, F., Nowlan, C., Rinsland, C. P.,
901 Rochon, Y. J., Rowlands, N., Semeniuk, K., Simon, P., Skelton, R., Sloan, J. J., Soucy, M.-
902 A., Strong, K., Tremblay, P., Turnbull, D., Walker, K. A., Walkty, I., Wardle, D. A.,

903 Wehrle, V., Zander, R., and Zou, J., Atmospheric Chemistry Experiment (ACE): Mission
904 overview, *Geophysical Research Letters*, 32, <https://doi.org/10.1029/2005GL022386>, 2005.

905 Boucher O., Servonnat, J., Albright, A. L., Aumont, O., Balkanski, Y., Bastrikov, V., et al.
906 (2020). Presentation and evaluation of the IPSL-CM6A-LR climate model. *Journal of*
907 *Advances in Modeling Earth Systems*, 12, e2019MS002010.
908 <https://doi.org/10.1029/2019MS002010>.

909 Bretherton, C. S., & Park, S. (2009). A new moist turbulence parameterization in the Community
910 Atmosphere Model. *Journal of Climate*, 22(12), 3422-3448.

911 Brodowsky, C., Sukhodolov, T., Feinberg, A., Höpfner, M., Peter, T., Stenke, A., & Rozanov, E.
912 (2021). Modeling the sulfate aerosol evolution after recent moderate volcanic activity,
913 2008–2012. *Journal of Geophysical Research: Atmospheres*, 126, e2021JD035472.
914 <https://doi.org/10.1029/2021JD035472>

915 Bruehl, C., Lelieveld, J., Schallrock, J., & Rieger, L. A. (2023, December). Chemistry Climate
916 Model Studies on the Effect of the Hunga Tonga Eruption on stratospheric Ozone in mid
917 and high Latitudes in 2022. In *AGU Fall Meeting Abstracts* (Vol. 2023, No. 2235, pp.
918 A21B-2235).

919 Carn, S., Clarisse, L., and Prata, A.: Multi-decadal satellite measurements of global volcanic
920 degassing, *J. Volcanol. Geoth. Res.*, 311, 99–134,
921 <https://doi.org/10.1016/j.jvolgeores.2016.01.002>, 2016.

922 Carn, S., Fioletov, V., McLinden, C. et al. A decade of global volcanic SO₂ emissions measured
923 from space. *Sci Rep* 7, 44095 (2017). <https://doi.org/10.1038/srep44095>

924 Carn, S. (2022), Multi-Satellite Volcanic Sulfur Dioxide L4 Long-Term Global Database V4,
925 Greenbelt, MD, USA, Goddard Earth Science Data and Information Services Center (GES
926 DISC), Accessed: [6/9/2024], 10.5067/MEASURES/SO2/DATA405

927 Case, P., Colarco, P. R., Toon, B., Aquila, V., & Keller, C. A. (2023). Interactive stratospheric
928 aerosol microphysics-chemistry simulations of the 1991 Pinatubo volcanic aerosols with
929 newly coupled sectional aerosol and stratosphere-troposphere chemistry modules in the
930 NASA GEOS Chemistry-Climate Model (CCM). *Journal of Advances in Modeling Earth*
931 *Systems*, 15(8), e2022MS003147.

932 Clyne, M., Lamarque, J.-F., Mills, M. J., Khodri, M., Ball, W., Bekki, S., Dhomse, S. S., Lebas,
933 N., Mann, G., Marshall, L., Niemeier, U., Poulain, V., Robock, A., Rozanov, E., Schmidt,
934 A., Stenke, A., Sukhodolov, T., Timmreck, C., Toohey, M., Tummon, F., Zanchettin, D.,
935 Zhu, Y., and Toon, O. B.: Model physics and chemistry causing intermodel disagreement
936 within the VolMIP-Tambora Interactive Stratospheric Aerosol ensemble, *Atmos. Chem.*
937 *Phys.*, 21, 3317–3343, <https://doi.org/10.5194/acp-21-3317-2021> , 2021.

938 Clyne, M.: Modeling the Role of Volcanoes in the Climate System – Chapter 4: Tonga-MIP,
939 Ph.D. dissertation, University of Colorado at Boulder, ProQuest Dissertations & Theses,
940 31487034, 153 pp., 2024.

941 Collins, W. J., Bellouin, N., Doutriaux-Boucher, M., Gedney, N., Halloran, P., Hinton, T., et al.
 942 Development and evaluation of an Earth-System model-HadGEM2. *Geoscientific Model*
 943 *Development*. <https://doi.org/10.5194/gmd-4-1051-2011>, 2011.

944 A. Collow, P. Colarco, A. da Silva, V. Buchard, H. Bian, M. Chin, S. Das, R. Govindaraju, D.
 945 Kim, V. Aquila: Benchmarking GOCART-2G in the Goddard Earth Observing System
 946 (GEOS), *Geoscientific Model Development*, 17, 1443–1468, doi: 10.5194/gmd-17-1443-
 947 2024 (2024).

948 Davis, N. A., Callaghan, P., Simpson, I. R., and Tilmes, S.: Specified dynamics scheme impacts
 949 on wave-mean flow dynamics, convection, and tracer transport in CESM2 (WACCM6),
 950 *Atmos. Chem. Phys.*, 22, 197–214, <https://doi.org/10.5194/acp-22-197-2022>, 2022.

951 Dennison, F., Keeble, J., Morgenstern, O., Zeng, G., Abraham, N. L. and Yang, X.:
 952 Improvements to stratospheric chemistry scheme in the UM-UKCA (v10.7) model: solar
 953 cycle and heterogeneous reactions, *Geosci. Mod. Dev.*, 12, 1227–1239, 2019.

954 Dhomse, S. S., Emmerson, K. M., Mann, G. W., Bellouin, N., Carslaw, K. S., Chipperfield, M.
 955 P. et al.: Aerosol microphysics simulations of the Mt. Pinatubo eruption with the UM-
 956 UKCA composition-climate model, *Atmos. Chem. Phys.*, 14, 11221–11246, 2014

957 Dhomse, S. S., Mann, G. W., Antuña Marrero, J. C., Shallcross, S. E., Chipperfield, M. P.,
 958 Carslaw, K. S., Marshall, L., Abraham, N. L., and Johnson, C. E.: Evaluating the simulated
 959 radiative forcings, aerosol properties, and stratospheric warmings from the 1963 Mt Agung,
 960 1982 El Chichón, and 1991 Mt Pinatubo volcanic aerosol clouds, *Atmos. Chem. Phys.*, 20,
 961 13627–13654, <https://doi.org/10.5194/acp-20-13627-2020>, 2020.

962 Duncan, B. N., Logan, J. A., Bey, I., Megretskaja, I. A., Yantosca, R. M., Novelli, P. C., ... &
 963 Rinsland, C. P. (2007). Global budget of CO, 1988–1997: Source estimates and validation
 964 with a global model. *Journal of Geophysical Research: Atmospheres*, 112(D22).

965 Gates, W. L., Boyle, J. S., Covey, C., Dease, C. G., Doutriaux, C. M., Drach, R. S., Fiorino, M.,
 966 Gleckler, P. J., Hnilo, J. J., Marlais, S. M., Phillips, T. J., Potter, G. L., Santer, B. D.,
 967 Sperber, K. R., Taylor, K. E., and Williams, D. N.: An Overview of the Results of the
 968 Atmospheric Model Intercomparison Project (AMIP I), *B. Am. Meteorol. Soc.*, 80, 29–55,
 969 1999.

970 English, J. M., Toon, O. B., Mills, M. J., and Yu, F.: Microphysical simulations of new particle
 971 formation in the upper troposphere and lower stratosphere, *Atmos. Chem. Phys.*, 11, 9303-
 972 9322, [10.5194/acp-11-9303-2011](https://doi.org/10.5194/acp-11-9303-2011), 2011.

973 English, J. M., Toon, O. B., & Mills, M. J. (2013). Microphysical simulations of large
 974 volcanic eruptions: Pinatubo and Toba. *Journal of Geophysical Research: Atmospheres*,
 975 118(4), 1880-1895.

976 Errera, Q., Chabrillat, S., Christophe, Y., Deboscher, J., Hubert, D., Lahoz, W., Santee, M. L.,
 977 Shiotani, M., Skachko, S., von Clarmann, T., and Walker, K.: Technical note: Reanalysis
 978 of Aura MLS chemical observations, *Atmos. Chem. Phys.*, 19, 13647–13679,
 979 <https://doi.org/10.5194/acp-19-13647-2019>, 2019.

980 Eskes, H., Tsikerdekis, A., Ades, M., Alexe, M., Benedictow, A. C., Bennouna, Y., Blake, L.,
 981 Bouarar, I., Chabrillat, S., Engelen, R., Errera, Q., Flemming, J., Garrigues, S., Griesfeller,
 982 J., Huijnen, V., Ilić, L., Inness, A., Kapsomenakis, J., Kipling, Z., Langerock, B., Mortier,
 983 A., Parrington, M., Pison, I., Pitkänen, M., Remy, S., Richter, A., Schoenhardt, A., Schulz,
 984 M., Thouret, V., Warneke, T., Zerefos, C., and Peuch, V.-H.: Technical note: Evaluation of
 985 the Copernicus Atmosphere Monitoring Service Cy48R1 upgrade of June 2023, *Atmos.*
 986 *Chem. Phys.*, 24, 9475–9514, <https://doi.org/10.5194/acp-24-9475-2024>, 2024.

987 Eyring, V., Cionni, I., Bodeker, G. E., Charlton-Perez, A. J., Kinnison, D. E., Scinocca, J. F., ...
 988 & Yamashita, Y. (2010). Multi-model assessment of stratospheric ozone return dates and
 989 ozone recovery in CCMVal-2 models. *Atmospheric Chemistry and Physics*, 10(19), 9451-
 990 9472. <https://doi.org/10.5194/acp-10-9451-2010>

991 Eyring, V., Bony, S., Meehl, G. A., Senior, C A., Stevens, B. et al., Overview of the Coupled
 992 Model Intercomparison Project Phase 6 (CMIP6) experimental design and organization,
 993 *Geosci. Model Dev.*, 9, 1937–1958, <https://doi.org/10.5194/gmd-9-1937-2016>, 2016

994 Fioletov, V., McLinden, C. A., Griffin, D., Abboud, I., Krotkov, N., Leonard, P. J. T., Li, C.,
 995 Joiner, J., Theys, N., and Carn, S. (2022), Multi-Satellite Air Quality Sulfur Dioxide (SO₂)
 996 Database Long-Term L4 Global V2, Edited by Peter Leonard, Greenbelt, MD, USA,
 997 Goddard Earth Science Data and Information Services Center (GES DISC), Accessed:
 998 [6/9/2024], 10.5067/MEASURES/SO2/DATA406

999 Fleming, E. L., Newman, P. A., Liang, Q., & Daniel, J. S. (2020). The impact of continuing
 1000 CFC-11 emissions on stratospheric ozone. *Journal of Geophysical Research: Atmospheres*,
 1001 125(3), e2019JD031849. <https://doi.org/10.1029/2019jd031849>

1002 Fleming, E. L., Newman, P. A., Liang, Q., & Oman, L. D. (2024). Stratospheric temperature and
 1003 ozone impacts of the Hunga Tonga-Hunga Ha'apai water vapor injection. *Journal of*
 1004 *Geophysical Research: Atmospheres*, 129(1), e2023JD039298.
 1005 <https://doi.org/10.1029/2023JD039298>

1006 Flemming, J., Huijnen, V., Arteta, J., Bechtold, P., Beljaars, A., Blechschmidt, A.-M.,
 1007 Diamantakis, M., Engelen, R. J., Gaudel, A., Inness, A., Jones, L., Josse, B., Katragkou, E.,
 1008 Marecal, V., Peuch, V.-H., Richter, A., Schultz, M. G., Stein, O., and Tsikerdekis, A.:
 1009 Tropospheric chemistry in the Integrated Forecasting System of ECMWF, *Geosci. Model*
 1010 *Dev.*, 8, 975–1003, 2015.685 <https://doi.org/10.5194/gmd-8-975-2015>

1011 Fomichev, V. I., Fu, C., de Grandpre, J., Beagley, S. R., Ogibalov, V. P., and McConnell, J. C.:
 1012 Model thermal response to minor radiative energy sources and sinks in the middle
 1013 atmosphere, *J. Geophys. Res.*, 109, D19107, doi:10.1029/2004JD004892, 2004.

1014 Gelaro, R., and Coauthors, 2017: The Modern-Era Retrospective Analysis for Research and
 1015 Applications, Version 2 (MERRA-2). *J. Climate*, 30, 5419–5454,
 1016 <https://doi.org/10.1175/JCLI-D-16-0758.1>.

1017 Gettelman, A., Mills, M. J., Kinnison, D. E., Garcia, R. R., Smith, A. K., Marsh, D. R., Tilmes,
 1018 S., Vitt, F., Bardeen, C. G., McNerney, J., Liu, H.-L., Solomon, S. C., Polvani, L. M.,
 1019 Emmons, L. K., Lamarque, J.-F., Richter, J. H., Glanville, A. S., Bacmeister, J. T., Phillips,

1020 A. S., Neale, R. B., Simpson, I. R., DuVivier, A. K., Hodzic, A., and Randel, W. J.: The
1021 Whole Atmosphere Community Climate Model Version6 (WACCM6), *J. Geophys. Res.-*
1022 *Atmos.*, 124, 12380–12403, <https://doi.org/10.1029/2019JD030943>, 2019.

1023 Gidden, M. J., Riahi, K., Smith, S. J., Fujimori, S., Luderer, G., Kriegler, E., ... & Takahashi, K.
1024 (2019). Global emissions pathways under different socioeconomic scenarios for use in
1025 CMIP6: a dataset of harmonized emissions trajectories through the end of the century.
1026 *Geoscientific model development*, 12(4), 1443-1475. [https://doi.org/10.5194/gmd-12-1443-](https://doi.org/10.5194/gmd-12-1443-2019)
1027 [2019](https://doi.org/10.5194/gmd-12-1443-2019)

1028 Grell, G. A., & Freitas, S. R. (2014). A scale and aerosol aware stochastic convective
1029 parameterization for weather and air quality modeling. *Atmospheric Chemistry and*
1030 *Physics*, 14(10), 5233-5250. <https://doi.org/10.5194/acp-14-5233-2014>

1031 Hersbach H, Bell B, Berrisford P, et al. (2020). The ERA5 global reanalysis. *Quarterly Journal*
1032 *of the Royal Meteorological Society*, 146: 1999–2049. <https://doi.org/10.1002/qj.3803>

1033 Hourdin, F., Musat, I., Bony, S., Braconnot, P., Codron, F., Dufresne, J.-L., Fairhead, L.,
1034 Filiberti, M.-A., Friedlingstein, P., Grandpeix, J.-Y., Krinner, G., Levan, P., Li, Z.-X., and
1035 Lott, F.. The LMDZ4 general circulation model : climate performance and sensitivity to
1036 parametrized physics with emphasis on tropical convection. *Climate Dynamics*, 27 :787–
1037 813, 2006.

1038 Huang, B., C. Liu, V. Banzon, E. Freeman, G. Graham, B. Hankins, T. Smith, and H.-M. Zhang,
1039 2020: Improvements of the Daily Optimum Interpolation Sea Surface Temperature
1040 (DOISST) Version 2.1, *Journal of Climate*, 34, 2923-2939. doi: 10.1175/JCLI-D-20-0166.1

1041 Huijnen, V., Flemming, J., Chabrillat, S., Errera, Q., Christophe, Y., Blechschmidt, A.-M.,
1042 Richter, A., and Eskes, H.: C-IFS-CB05-BASCOE: stratospheric chemistry in the
1043 Integrated Forecasting System of ECMWF, *Geoscientific Model Development*, 9, 3071–
1044 3091, 2016.705

1045 Hurrell, J. W., et al. (2013), The community Earth system model: A framework for collaborative
1046 research, *Bull. Am. Meteorol. Soc.*, doi:10.1175/ BAMS-D-12-00121.

1047 Iacono, M. J., Delamere, J. S., Mlawer, E. J., Shephard, M. W., Clough, S. A., & Collins, W. D.
1048 (2008). Radiative forcing by long-lived greenhouse gases: Calculations with the AER
1049 radiative transfer models. *Journal of Geophysical Research: Atmospheres*, 113(D13).

1050 Jöckel, P., Kerkweg, A., Pozzer, A., Sander, R., Tost, H., Riede, H., Baumgaertner, A., Gromov,
1051 S., and Kern, B.: Development cycle 2 of the Modular Earth Submodel System (MESSy2),
1052 *Geosci. Model Dev.*, 3, 717–752, 2010.

1053 Jones, A. C., J. M. Haywood, A. Jones, V. Aquila. Sensitivity of volcanic aerosol dispersion to
1054 meteorological conditions: a Pinatubo case study, *J. Geophys. Res.*, 121(12), 6892-6908,
1055 doi: 10.1002/2016JD025001, 2016.

1056 Jonsson, A. I., de Grandpré, J., Fomichev, V. I., McConnell, J. C., and Beagley, S. R., Doubled
1057 CO₂-induced cooling in the middle atmosphere: Photochemical analysis of the ozone
1058 radiative feedback, *J. Geophys. Res.*, 109, D24103, doi:10.1029/2004JD005093, 2004.

1059 Kawamiya, M., Hajima, T., Tachiiri, K. et al. Two decades of Earth system modeling with an
1060 emphasis on Model for Interdisciplinary Research on Climate (MIROC). *Prog Earth Planet*
1061 *Sci* 7, 64. <https://doi.org/10.1186/s40645-020-00369-5>, (2020).

1062 Kleinschmitt, C., Boucher, O., Bekki, S., Lott, F., and Platt, U.: The Sectional Stratospheric
1063 Sulfate Aerosol module (S3A-v1) within the LMDZ general circulation model: description
1064 and evaluation against stratospheric aerosol observations, *Geosci. Model Dev.*, 10, 3359–
1065 3378, 2017, <https://doi.org/10.5194/gmd-10-3359-2017>.

1066 Kohl, M., C. Brühl, J. Schallock, H. Tost, P. Jöckel, A. Jost, S. Beirle, M. Höpfner, and A.
1067 Pozzer (2024). New submodel for emissions from Explosive Volcanic ERuptions (EVER
1068 v1.1) within the Modular Earth Submodel System (MESSy, version 2.55.1),
1069 <https://doi.org/10.5194/egusphere-2024-2200>.

1070 Kovilakam, M., Thomason, L. W., Ernest, N., Rieger, L., Bourassa, A., and Millán, L. (2020),
1071 The Global Space-based Stratospheric Aerosol Climatology (version 2.0): 1979–2018,
1072 *Earth Syst. Sci. Data*, 12, 2607–2634, <https://doi.org/10.5194/essd-12-2607-2020>.

1073 Kovilakam, M., Thomason, L., and Knepp, T.: SAGE III/ISS aerosol/cloud categorization and its
1074 impact on GloSSAC, *Atmos. Meas. Tech.*, 16, 2709–2731, [https://doi.org/10.5194/amt-16-](https://doi.org/10.5194/amt-16-2709-2023)
1075 [2709-2023](https://doi.org/10.5194/amt-16-2709-2023), 2023.

1076 Kuhlbrodt, T., Jones, C. G., Sellar, A., Storkey, D., Blockley, E., Stringer, M., et al. (2018). The
1077 Low-Resolution Version of HadGEM3 GC3.1: Development and Evaluation for Global
1078 Climate. *Journal of Advances in Modeling Earth Systems*, 10, 2865–2888.
1079 <https://doi.org/10.1029/2018MS001370>, 2018.

1080 Lamarque, J.-F., et al. (2012), CAM-chem: Description and evaluation of interactive atmospheric
1081 chemistry in the Community Earth System Model, *Geosci. Model Dev.*, 5(2), 369–411,
1082 [doi:10.5194/gmd-5-369-2012](https://doi.org/10.5194/gmd-5-369-2012).

1083 Lefèvre, F., Brasseur, G. P., Folkins, I., Smith, A. K., and Simon, P.: Chemistry of the 1991–
1084 1992 stratospheric winter: Three-dimensional model simulations, *J. Geophys. Res.-Atmos.*,
1085 99, 8183–8195, <https://doi.org/10.1029/93JD03476>, 1994.

1086 Lefèvre, F., Figarol, F., Carslaw, K. S., and Peter, T.: The 1997 Arctic Ozone depletion
1087 quantified from three-dimensional model simulations, *Geophys. Res. Lett.*, 25, 2425–2428,
1088 <https://doi.org/10.1029/98GL51812>, 1998.

1089 Jörmann, A., 2024. REMAP-GloSSAC-2023 [dataset]. ETH Zürich, url:
1090 <http://hdl.handle.net/20.500.11850/713396>. doi: 10.3929/ethz-b-000713396.

1091 Li, C., Peng, Y., Asher, E., Baron, A. A., Todt, M., Thornberry, T. D., et al. (2024).
1092 Microphysical simulation of the 2022 Hunga volcano eruption using a sectional aerosol
1093 model. *Geophysical Research Letters*, 51, e2024GL108522.
1094 <https://doi.org/10.1029/2024GL108522>

1095 Lin, S. J., & Rood, R. B. (1996). Multidimensional flux-form semi-Lagrangian transport
1096 schemes. *Monthly weather review*, 124(9), 2046-2070. [https://doi.org/10.1175/1520-](https://doi.org/10.1175/1520-0493(1996)124%3C2046:MFFSLT%3E2.0.CO;2)
1097 [0493\(1996\)124%3C2046:MFFSLT%3E2.0.CO;2](https://doi.org/10.1175/1520-0493(1996)124%3C2046:MFFSLT%3E2.0.CO;2)

1098 Liu, X., Easter, R. C., Ghan, S. J., Zaveri, R., Rasch, P., Shi, X., Lamarque, J.-F., Gettelman, A.,
1099 Morrison, H., Vitt, F., Conley, A., Park, S., Neale, R., Hannay, C., Ekman, A. M. L., Hess,
1100 P., Mahowald, N., Collins, W., Iacono, M. J., Bretherton, C. S., Flanner, M. G., and
1101 Mitchell, D.: Toward a minimal representation of aerosols in climate models: description
1102 and evaluation in the Community Atmosphere Model CAM5, *Geosci. Model Dev.*, 5, 709–
1103 739, <https://doi.org/10.5194/gmd-5-709-2012>, 2012.

1104 Liu, X., Ma, P.-L., Wang, H., Tilmes, S., Singh, B., Easter, R. C., Ghan, S. J., and Rasch, P. J.:
1105 Description and evaluation of a new four-mode version of the Modal Aerosol Module
1106 (MAM4) within version 5.3 of the Community Atmosphere Model, *Geosci. Model Dev.*, 9,
1107 505–522, <https://doi.org/10.5194/gmd-9-505-2016>, 2016.

1108 Lock, A. P., Brown, A. R., Bush, M. R., Martin, G. M., & Smith, R. N. B. (2000). A new
1109 boundary layer mixing scheme. Part I: Scheme description and single-column model tests.
1110 *Monthly weather review*, 128(9), 3187-3199.

1111 Lurton, T., Balkanski, Y., Bastrikov, V., Bekki, S., Bopp, L., Braconnot, P., et al. (2020).
1112 Implementation of the CMIP6 forcing data in the IPSL-CM6A-LR model. *Journal of*
1113 *Advances in Modeling Earth Systems*, 12, e2019MS001940.
1114 <https://doi.org/10.1029/2019MS001940>

1115 Mann, G. W., Carslaw, K. S., Spracklen, D. V., Ridley, D. A., Manktelow, P. T., Chipperfield,
1116 M. P., Pickering, S. J. and Johnson, C. E.: Description and evaluation of GLOMAP-mode:
1117 a modal global aerosol microphysics model for the UKCA composition-climate model
1118 *Geosci. Mod. Dev.*, 3, 519-551, <https://doi.org/10.5194/gmd-3-519-2010>, 2010.

1119 Mann, G. W. , Carslaw, K. S., Spracklen, D. V., Pringle, K. J., Merikanto, J., Korhonen, H. et al..
1120 Intercomparison of modal and sectional aerosol microphysics representations within the
1121 same 3-D global chemical transport model, *Atmos. Chem. Phys.*, 12, 4449–4476, 2012.

1122 Marchand, M., Keckhut, P., Lefebvre, S., Claud, C., Cugnet, D., Hauchecorne, A., et al. (2012).
1123 Dynamical amplification of the stratospheric solar response simulated with the Chemistry-
1124 Climate Model LMDz-Reprobus. *Journal of Atmospheric and Solar-Terrestrial Physics*,
1125 75–76, 147–160. <https://doi.org/10.1016/j.jastp.2011.11.008>

1126 Mills, M. J., O. B. Toon, V. Vaida, P. E. Hintze, H. G. Kjaergaard, D. P. Schofield, and T. W.
1127 Robinson (2005), Photolysis of sulfuric acid vapor by visible light as a source of the polar
1128 stratospheric CN layer, *J. Geophys. Res.*, 110, D08201, doi:10.1029/2004JD005519.

1129 Mills, M. J., Schmidt, A., Easter, R., Solomon, S., Kinnison, D. E., Ghan, S. J., Neely, R. R.,
1130 Marsh, D. R., Conley, A., Bardeen, C. G., and Gettelman, A.: Global volcanic aerosol
1131 properties derived from emissions, 1990–2014, using CESM1(WACCM), *J. Geophys.*
1132 *Res.-Atmos.*, 121, 2332–2348, <https://doi.org/10.1002/2015JD024290>, 2016.

1133 Mills, M. J., Richter, J. H., Tilmes, S., Kravitz, B., Mac-Martin, D. G., Glanville, A. A., Tribbia,
1134 J. J., Lamarque, J.-F., Vitt, F., Schmidt, A., Gettelman, A., Hannay, C., Bacmeister, J. T.,
1135 and Kinnison, D. E.: Radiative and chemical response to interactive stratospheric sulfate
1136 aerosols in fully coupled CESM1(WACCM), *J. Geophys. Res.-Atmos.*, 122, 13061–13078,
1137 <https://doi.org/10.1002/2017JD027006>, 2017.

1138 Molod, A., Takacs, L., Suarez, M., and Bacmeister, J.: Development of the GEOS-5 atmospheric
1139 general circulation model: evolution from MERRA to MERRA2, *Geosci. Model Dev.*, 8,
1140 1339-1356, [10.5194/gmd-8-1339-2015](https://doi.org/10.5194/gmd-8-1339-2015), 2015.

1141 Morgenstern, O., Braesicke, P., O'Connor, F. M., Bushell, A. C., Johnson, C. E., Osprey, S. M.
1142 and Pyle, J. A. : Evaluation of the new UKCA climate-composition model – Part 1: The
1143 stratosphere, *Geosci. Mod. Dev.*, 2, 43-57, <https://doi.org/10.5194/gmd-2-43-2009>, 2009.

1144 Morgenstern, O., Hegglin, M. I., Rozanov, E., O'Connor, F. M., Abraham, N. L., Akiyoshi, H., ...
1145 & Zeng, G. (2017). Review of the global models used within phase 1 of the Chemistry–
1146 Climate Model Initiative (CCMI). *Geoscientific Model Development*, 10(2), 639-671.

1147 Mulcahy, J. P., Jones, C., Sellar, A., Johnson, B., Boutle, I. A., Jones, A., Andrews T. et al.
1148 Improved Aerosol Processes and Effective Radiative Forcing in HadGEM3 and UKESM1,
1149 *Journal of Advances in Modeling Earth Systems*, 10, 2786–2805.
1150 <https://doi.org/10.1029/2018MS001464>, 2018.

1151 Mulcahy, J. P., Johnson, C., Jones, C. G., Povey, A. C., Scott, C. E., Sellar, A., Turnock, S. T. et
1152 al.: Description and evaluation of aerosol in UKESM1 and HadGEM3-GC3.1 CMIP6
1153 historical simulations, *Geosci. Model Dev.*, 13, 6383–6423, [https://doi.org/10.5194/gmd-](https://doi.org/10.5194/gmd-13-6383-2020)
1154 [13-6383-2020](https://doi.org/10.5194/gmd-13-6383-2020), 2020.

1155 Mulcahy, J. P., Jones, C. G., Rumbold, S. Kuhlbrodt, T., Dittus, A. J. Blockley, E. W. et al., :
1156 UKESM1.1: development and evaluation of an updated configuration of the UK Earth
1157 System Model, *Geosci. Model Dev.*, 16, 1569–1600, [https://doi.org/10.5194/gmd-16-1569-](https://doi.org/10.5194/gmd-16-1569-2023)
1158 [2023](https://doi.org/10.5194/gmd-16-1569-2023), 2023

1159 Naujokat, B., An update of the observed Quasi-Biennial Oscillation of the stratospheric winds
1160 over the tropics, *J. Atmos. Sci.*, 43, 1873 - 1877, [https://doi.org/10.1175/1520-](https://doi.org/10.1175/1520-0469(1986)043<1873:AUOTOQ>2.0.CO;2)
1161 [0469\(1986\)043<1873:AUOTOQ>2.0.CO;2](https://doi.org/10.1175/1520-0469(1986)043<1873:AUOTOQ>2.0.CO;2), 1986.

1162 Neely III, Ryan R. and Schmidt, Anja (2016) *VolcanEESM: Global volcanic sulphur dioxide*
1163 *(SO₂) emissions database from 1850 to present*. Centre for Environmental Data Analysis.
1164 [Dataset] <https://doi.org/10.5285/76ebdc0b-0eed-4f70-b89e-55e606bcd568>

1165 O'Connor, F. M., Johnson, C. E., Morgenstern, O., Abraham, N. L., Braesicke, P. et al.:
1166 Evaluation of the new UKCA climate-composition model– Part 2: The Troposphere,
1167 *Geosci. Model Dev.*, 7, 41–91, <https://doi.org/10.5194/gmd-7-41-2014>, 2014.

1168 O'Neill, B.C., Tebaldi, C., van Vuuren, D.P., et al., The Scenario Model Intercomparison Project
1169 (ScenarioMIP) for CMIP6. *Geoscientific Model Development*, 9, 9, 3461–3482,
1170 doi:10.5194/gmd-9-3461-2016, 2016.

1171 Nielsen, J. E., Pawson, S., Molod, A., Auer, B., Da Silva, A. M., Douglass, A. R., ... & Wargan,
1172 K. (2017). Chemical mechanisms and their applications in the Goddard Earth Observing
1173 System (GEOS) earth system model. *Journal of Advances in Modeling Earth Systems*, 9(8),
1174 3019-3044.

1175 Peuch, V.-H., Engelen, R., Rixen, M., Dee, D., Flemming, J., Suttie, M., Ades, M., Agusti-
1176 Panareda, A., Ananasso, C., Andersson, E., Armstrong, D., Barre, J., Bousserez, N.,
1177 Dominguez, J. J., Garrigues, S., Inness, A., Jones, L., Kipling, Z., Letertre-Danczak, J.,

1178 Parrington, M., Razinger, M., Ribas, R., Vermoote, S., Yang, X., Simmons, A., de
1179 Marcilla, J. G., and Thepaut, J.-N.: The Copernicus Atmosphere Monitoring Service: From
1180 Research to Operations, *Bulletin of the American Meteorological Society*, 103, E2650 –
1181 E2668, <https://doi.org/10.1175/BAMS-D-21-0314.1>, 2022.

1182 Pringle, K. J., Tost, H., Message, S., Steil, B., Giannadaki, D., Nenes, A., Fountoukis, C., Stier,
1183 P., Vignati, E., and Lelieveld, J.: Description and evaluation of GMXe: a new aerosol
1184 submodel for global simulations (v1), *Geosci. Model Dev.*, 3, 391–412, 2010.

1185 Putman, W. M., & Lin, S. J. (2007). Finite-volume transport on various cubed-sphere grids.
1186 *Journal of Computational Physics*, 227(1), 55-78.

1187 Quaglia, I., Timmreck, C., Niemeier, U., Vioni, D., Pitari, G., Brodowsky, C., Brühl, C.,
1188 Dhomse, S. S., Franke, H., Laakso, A., Mann, G. W., Rozanov, E., and Sukhodolov, T.:
1189 Interactive stratospheric aerosol models' response to different amounts and altitudes of SO2
1190 injection during the 1991 Pinatubo eruption, *Atmos. Chem. Phys.*, 23, 921–948,
1191 <https://doi.org/10.5194/acp-23-921-2023>, 2023.

1192 Randel, W. J., Wang, X., Starr, J., Garcia, R. R., & Kinnison, D. (2024). Long-term temperature
1193 impacts of the Hunga volcanic eruption in the stratosphere and above. *Geophysical*
1194 *Research Letters*, 51, e2024GL111500. <https://doi.org/10.1029/2024GL111500>

1195 Reinecker, M., Suarez, M., Todling, R., Bacmeister, J., Takacs, L., & Liu, H. (2008). The
1196 GEOS-5 data assimilation system-documentation of versions 5.0. 1, 5.1. 0 (No. NASA
1197 Tech Rep TM-2007, 104606).

1198 Rémy, S., Kipling, Z., Huijnen, V., Flemming, J., Nabat, P., Michou, M., Ades, M., Engelen, R.,
1199 and Peuch, V.-H.: Description and evaluation of the tropospheric aerosol scheme in the
1200 Integrated Forecasting System (IFS-AER, cycle 47R1) of ECMWF, *Geoscientific Model*
1201 *Development*, 15, 4881–4912, <https://doi.org/10.5194/gmd-15-4881-2022>, 2022.

1202 Reynolds, R. W., N. A. Rayner, T. M. Smith, D. C. Stokes, and W. Wang, 2002: An Improved In
1203 Situ and Satellite SST Analysis for Climate. *J. Climate*, 15, 1609–1625,
1204 [https://doi.org/10.1175/1520-0442\(2002\)015<1609:AIISAS>2.0.CO;2](https://doi.org/10.1175/1520-0442(2002)015<1609:AIISAS>2.0.CO;2).

1205 Schallock, J., C. Brühl, C. Bingen, M. Höpfner, L. Rieger, and J. Lelieveld (2023),
1206 Reconstructing volcanic radiative forcing since 1990, using a comprehensive emission
1207 inventory and spatially resolved sulfur injections from satellite data in a chemistry-climate
1208 model, *Atmos. Chem. Phys.*, 23, 1169–1207.

1209 Scinocca, J. F.: An Accurate Spectral Non-Orographic Gravity Wave Parameterization for
1210 General Circulation Models, *J. Atmos. Sci.*, 60, 667–682, [https://doi.org/10.1175/1520-0469\(2003\)060%3C0667:AASNGW%3E2.0.CO;2](https://doi.org/10.1175/1520-0469(2003)060%3C0667:AASNGW%3E2.0.CO;2), 2003.

1212 Scinocca, J. F., McFarlane, N. A., Lazare, M, Li, J., and Plummer, D., Technical Note: The
1213 CCCma third generation AGCM and its extension into the middle atmosphere, *Atmos.*
1214 *Chem. Phys.*, 8, 7055–7074, <https://doi.org/10.5194/acp-8-7055-2008>, 2008.

1215 Seddon, J., Stephens, A., Mizielinski, M. S., Vidale, P. L., and Roberts, M. J.: Technology to aid
1216 the analysis of large-volume multi-institute climate model output at a central analysis

1217 facility (PRIMAVERA Data Management Tool V2.10), *Geosci. Model Dev.*, 16, 6689–
1218 6700, <https://doi.org/10.5194/gmd-16-6689-2023>, 2023.

1219 Sekiya, T., K. Sudo, and T. Nagai (2016), Evolution of stratospheric sulfate aerosol from the
1220 1991 Pinatubo eruption: Roles of aerosol microphysical processes, *J. Geophys. Res.*
1221 *Atmos.*, 121, 2911–2938, doi:10.1002/2015JD024313.

1222 Sellar, A., J., C. G. Jones, J. Mulcahy, Y. Tang et al. (2019), UKESM1: Description and
1223 Evaluation of the U.K. Earth System Model, *J. Adv. Mod. Earth Systems*, 11, 4513-4558,
1224 <https://doi.org/10.1029/2019MS001739>

1225 Sellar, A., J. Walton, C. G. Jones, R. Wood et al. (2020), Implementation of U.K. Earth System
1226 Models for CMIP6, *J. Adv. Mod. Earth Systems*, 12, e2019MS001946.
1227 <https://doi.org/10.1029/2019MS001946>

1228 Strahan, S. E., Duncan, B. N., & Hoor, P. (2007). Observationally derived transport diagnostics
1229 for the lowermost stratosphere and their application to the GMI chemistry and transport
1230 model. *Atmospheric Chemistry and Physics*, 7(9), 2435-2445.

1231 Sukhodolov, T., Egorova, T., Stenke, A., Ball, W. T., Brodowsky, C., Chiodo, G., Feinberg, A.,
1232 Friedel, M., Karagodin-Doyennel, A., Peter, T., Sedlacek, J., Vattioni, S., and Rozanov, E.:
1233 Atmosphere ocean aerosol chemistry climate model SOCOLv4.0: description and
1234 evaluation, *Geosci. Model Dev.*, 14, 5525–5560, [https://doi.org/10.5194/gmd-14-5525-](https://doi.org/10.5194/gmd-14-5525-2021)
1235 [2021](https://doi.org/10.5194/gmd-14-5525-2021) , 2021.

1236 Taha, G., et al. (2021), OMPS LP Version 2.0 multi-wavelength aerosol extinction coefficient
1237 retrieval algorithm, *Atmospheric Measurement Techniques*, 14,
1238 <https://doi.org/10.5194/amt-14-1015-2021>

1239 Taha, G., et al. "Tracking the 2022 Hunga Tonga-Hunga Ha'apai aerosol cloud in the upper and
1240 middle stratosphere using space-based observations." *Geophysical Research Letters* 49.19
1241 (2022): e2022GL100091.

1242 Tilmes, S., Mills, M. J., Zhu, Y., Bardeen, C. G., Vitt, F., Yu, P., Fillmore, D., Liu, X., Toon, B.,
1243 and Deshler, T.: Description and performance of a sectional aerosol microphysical model
1244 in the Community Earth System Model (CESM2), *Geosci. Model Dev.*, 16, 6087-6125,
1245 [10.5194/gmd-16-6087-2023](https://doi.org/10.5194/gmd-16-6087-2023), 2023. doi: 10.5194/gmd-16-6087-2023

1246 Tatebe, H., Ogura, T., Nitta, T., Komuro, Y., Ogochi, K., Takemura, T., Sudo, K., Sekiguchi, M.,
1247 Abe, M., Saito, F., Chikira, M., Watanabe, S., Mori, M., Hirota, N., Kawatani, Y.,
1248 Mochizuki, T., Yoshimura, K., Takata, K., O'ishi, R., Yamazaki, D., Suzuki, T., Kurogi,
1249 M., Kataoka, T., Watanabe, M., and Kimoto, M.: Description and basic evaluation of
1250 simulated mean state, internal variability, and climate sensitivity in MIROC6, *Geosci.*
1251 *Model Dev.*, 12, 2727–2765, <https://doi.org/10.5194/gmd-12-2727-2019>, 2019.

1252 Telford, P., Braesicke, P., Morgenstern, O. and Pyle, J. : Technical Note: Description and
1253 assessment of a nudged version of the new dynamics Unified Model, *Atmos. Chem. Phys.*,
1254 8, 1701–1712, <https://doi.org/10.5194/acp-8-1701-2008>, 2008.

1255 Telford, P., Braesicke, P., Morgenstern, O. and Pyle, J. : Reassessment of causes of ozone
1256 column variability following the eruption of Mount Pinatubo using a nudged CCM, *Atmos.*
1257 *Chem. Phys.*, 9, 4251–4260, <https://doi.org/10.5194/acp-9-4251-2009>, 2009.

1258 Tsujino, H. et al. JRA-55 based surface dataset for driving ocean–sea-ice models (JRA55-do).
1259 *Ocean Modell.* 130, 79–139 (2018).

1260 Thomason, L. W., N. Ernest, L. Millán, L. Rieger, A. Bourassa, J.-P. Vernier, G. Manney, T.
1261 Peter, B. Luo, and F. Arfeuille (2018), A global, space-based stratospheric aerosol
1262 climatology: 1979 to 2016, *Earth System Science Data*, 10, 469–492,
1263 <https://doi.org/10.5194/essd-10-469-2018>.

1264 Vehkamäki, H., Kulmala, M., Napari, I., Lehtinen, K. E., Timmreck, C., Noppel, M., and
1265 Laaksonen, A.: An improved parameterization for sulfuric acid-water nucleation rates for
1266 tropospheric and stratospheric conditions, *J. Geophys. Res.-Atmos.*, 107, AAC 3- 1–AAC
1267 3-10, <https://doi.org/10.1029/2002JD002184>, 2002.

1268 Walters, D., Baran, A. J. Boutle, I., Brooks, M., Earnshaw, P., Edwards, J., Furtado, K., Hill, P.
1269 et al. The Met Office Unified Model Global Atmosphere 7.0/7.1 and JULES Global Land
1270 7.0 configurations, *Geosci. Model Dev.*, 12, 1909–1963, 2019.

1271 Wang, X., Randel, W., Zhu, Y., Tilmes, S., Starr, J., Yu, W., et al. (2023). Stratospheric climate
1272 anomalies and ozone loss caused by the Hunga Tonga-Hunga Ha'apai volcanic eruption.
1273 *Journal of Geophysical Research: Atmospheres*, 128, e2023JD039480.
1274 <https://doi.org/10.1029/2023JD039480>

1275 Watanabe, S., Hajima, T., Sudo, K., Nagashima, T., Takemura, T., Okajima, H., Nozawa, T.,
1276 Kawase, H., Abe, M., Yokohata, T., Ise, T., Sato, H., Kato, E., Takata, K., Emori, S., and
1277 Kawamiya, M.: MIROC-ESM 2010: model description and basic results of CMIP5-20c3m
1278 experiments, *Geosci. Model Dev.*, 4, 845–872, <https://doi.org/10.5194/gmd-4-845-2011>,
1279 2011.

1280 Williams K. D., Copsey, D., Blockley, E.W., Bodas-Salcedo, A., Calvert, D., Comer, R., et al.
1281 (2018). The Met Office Global Coupled Model 3.0 and 3.1 (GC3.0 and GC3.1)
1282 Configurations. *Journal of Advances in Modeling Earth Systems*, 10(2), 357–380.
1283 <https://doi.org/10.1002/2017MS001115> (2018)

1284 Williams, J. E., Huijnen, V., Bouarar, I., Meziane, M., Schreurs, T., Pelletier, S., Marecal, V.,
1285 Josse, B., and Flemming, J.: Regional evaluation of the performance of the global CAMS
1286 chemical modeling system over the United States (IFS cycle 47r1), *Geoscientific Model*
1287 *Development*, 15, 4657–4687, <https://doi.org/10.5194/gmd-15-4657-2022>, 2022.

1288 Wood, N., Staniforth, A., White, A., Allen, T., Diamantakis, M., Gross, M., Melvin, T., Smith,
1289 C., Vosper, S., Zerroukat, M., and Thuburn, J.: An inherently mass-conserving semi-
1290 implicit semi-Lagrangian discretization of the deep-atmosphere global nonhydrostatic
1291 equations, *Q. J. Roy. Meteorol. Soc.*, 140, 1505–1520, <https://doi.org/10.1002/qj.2235>,
1292 2014.

1293 Yu, P., O. B. Toon, C. G. Bardeen, M. J. Mills, T. Fan, J. M. English, and R. R. Neely (2015),
1294 Evaluations of tropospheric aerosol properties simulated by the community earth system

1295 model with a sectional aerosol microphysics scheme, *J. Adv. Model. Earth Syst.*, 7, 865–
1296 914, doi:10.1002/2014MS000421.

1297 Yu, W., Garcia, R., Yue, J., Smith, A., Wang, X., Randel, W., ... & Mlynczak, M. (2023).
1298 Mesospheric temperature and circulation response to the Hunga Tonga-Hunga-Ha'apai
1299 volcanic eruption. *Journal of Geophysical Research: Atmospheres*, 128(21),
1300 e2023JD039636.

1301 Zhang, J., Kinnison, D., Zhu, Y., Wang, X., Tilmes, S., Dube, K., & Randel, W. (2024).
1302 Chemistry contribution to stratospheric ozone depletion after the unprecedented water-rich
1303 Hunga Tonga eruption. *Geophysical Research Letters*, 51, e2023GL105762.
1304 <https://doi.org/10.1029/2023GL105762>

1305 Zhou, X., S.S. Dhomse, W. Feng, G. Mann, S. Heddell, H. Pumphrey, B.J. Kerridge, B. Latter,
1306 R. Siddans, L. Ventress, R. Querel, P. Smale, E. Asher, E.G. Hall, S. Bekki and M.P.
1307 Chipperfield (2024), Antarctic vortex dehydration in 2023 as a substantial removal
1308 pathway for Hunga Tonga-Hunga Ha'apai water vapour, *Geophysical Research Letters*, 51,
1309 e2023GL107630, doi:10.1029/2023GL107630.

1310 Zhu, Y., Bardeen, C.G., Tilmes, S. et al. Perturbations in stratospheric aerosol evolution due to
1311 the water-rich plume of the 2022 Hunga-Tonga eruption. *Commun Earth Environ* 3, 248
1312 (2022). <https://doi.org/10.1038/s43247-022-00580-w>